

Assessment of the GLLB-SC potential for solid-state properties and attempts for improvement

Fabien Tran, Sohaib Ehsan, and Peter Blaha
*Institute of Materials Chemistry, Vienna University of Technology,
Getreidemarkt 9/165-TC, A-1060 Vienna, Austria*

Based on the work of Gritsenko *et al.* (GLLB) [Phys. Rev. A **51**, 1944 (1995)], the method of Kuisma *et al.* [Phys. Rev. B **82**, 115106 (2010)] to calculate the band gap in solids was shown to be much more accurate than the common local density approximation (LDA) and generalized gradient approximation (GGA). The main feature of the GLLB-SC potential (SC stands for solid and correlation) is to lead to a nonzero derivative discontinuity that can be conveniently calculated and then added to the Kohn-Sham band gap for a comparison with the experimental band gap. In this work, a thorough comparison of GLLB-SC with other methods, e.g., the modified Becke-Johnson (mBJ) potential [F. Tran and P. Blaha, Phys. Rev. Lett. **102**, 226401 (2009)], for electronic, magnetic, and density-related properties is presented. It is shown that for the band gap, GLLB-SC does not perform as well as mBJ for systems with a small band gap and strongly correlated systems, but is on average of similar accuracy as hybrid functionals. The results on itinerant metals indicate that GLLB-SC overestimates significantly the magnetic moment (much more than mBJ does), but leads to excellent results for the electric field gradient, for which mBJ is in general not recommended. In the aim of improving the results, variants of the GLLB-SC potential are also tested.

I. INTRODUCTION

The great success of the Kohn-Sham (KS) density functional theory (DFT) method^{1,2} for the calculation of properties of electronic systems is due to the fact that in many circumstances, results of sufficient accuracy can be obtained at much lower cost compared to the supposedly more reliable post-Hartree-Fock³ or Green's function based methods.⁴ However, in KS-DFT the exchange (x) and correlation (c) effects are approximated and among the hundreds of approximations available,⁵ one has to choose an appropriate one for the system at hand. This choice is crucial when the trends in the results may depend significantly on the approximation, but the main problem is that it is by far not always obvious which approximation to choose. Therefore, the search for approximations that are more broadly accurate is a very active research topic,⁶⁻⁹ in particular since KS-DFT is used in many areas of science.

The focus of the present work is on the properties which depend directly on the xc potential $v_{xc,\sigma}$ (σ is the spin index) in the KS equations, namely, the electronic structure, magnetic moment, and electron density. Given an xc energy functional E_{xc} , the variational principle requires $v_{xc,\sigma}$ to be the functional derivative of E_{xc} . Depending on the type of approximation chosen for E_{xc} and the way the functional derivative is taken (with respect to the electron density ρ_σ or the orbitals $\psi_{i\sigma}$), the potential $v_{xc,\sigma}$ can be of different nature: multiplicative or nonmultiplicative.^{6,10} Strictly speaking, the potential $v_{xc,\sigma}$ in the KS method is multiplicative, while the generalized KS framework¹¹ (gKS) includes also nonmultiplicative potentials.

It is well-known that with the *exact multiplicative potential*, the KS band gap E_g^{KS} , defined as the conduction band minimum (CBM) minus the valence band maximum (VBM), is not equal to the true experimental (i.e.,

quasi-particle) band gap $E_g = I - A$ (ionization potential I minus electron affinity A) since they differ by the so-called xc derivative discontinuity Δ_{xc} ,^{12,13}

$$E_g = E_g^{\text{KS}} + \Delta_{xc}, \quad (1)$$

which can be of the same order of magnitude as the gap.¹⁴⁻¹⁷ Since Δ_{xc} is positive, the exact KS gap E_g^{KS} is (much) smaller than E_g . Therefore, within the KS framework a comparison with the experimental gap should formally be done only when Δ_{xc} is added to the KS band gap. With the functionals of the local density approximation (LDA) and generalized gradient approximation (GGA) that are commonly used for structure optimization or binding energy calculation (e.g., PBE¹⁸), E_g^{KS} is usually much smaller than E_g (see, e.g., Ref. 19), while adding Δ_{xc} (calculated in some way, which is possible for finite systems²⁰⁻²²) improves the agreement with experiment. Note that interestingly, the LDA and standard GGA methods lead to KS band gaps that do not differ that much from accurate KS band gaps.¹⁴⁻¹⁷

Semilocal multiplicative xc potentials that are more useful for band gap calculation have been proposed,²³⁻³³ however since usually this is still E_g^{KS} that is compared to the experimental value of E_g (no Δ_{xc} added to E_g^{KS}), the better agreement is achieved at the cost of having a potential v_{xc} that may show features that are most likely unphysical and not present in the exact KS potential (see, e.g., Fig. 2 of Ref. 34). Then, this may possibly lead to a bad description of properties other than the band gap. For instance, the modified Becke-Johnson (mBJ) potential,²⁸ which has been very successful for band gap prediction,³⁴⁻⁴² has also shown to be sometimes rather inaccurate for other properties, e.g., band widths⁴² or the magnetic moment of itinerant metals.⁴³ This is the consequence of constructing a potential that is not well-founded from the physical point of view.

Thus, when using a multiplicative potential the proper calculation of $E_g = I - A$ should consist of a nonzero derivative discontinuity that is added to E_g^{KS} [Eq. (1)]. In Refs. 20–22, and 44, methods to calculate the derivative discontinuity were proposed, however among these works only the one from Kuisma *et al.*⁴⁴ can be used for solids. They showed how to calculate the exchange part Δ_x of the derivative discontinuity from quantities that are obtained from a standard ground-state KS calculation. Δ_x is nonzero since they used a xc potential that is based on the one proposed by Gritsenko *et al.* (GLLB),^{45,46} which exhibits a jump (step structure) when the lowest unoccupied orbital starts to be occupied. The GLLB potential is a simplified version of the Krieger-Li-Iafrate (KLI) approximation⁴⁷ to the optimized effective potential (OEP).⁴⁸ The potential of Kuisma *et al.*,⁴⁴ called GLLB-SC (SC for solid and correlation), has been shown to be much more accurate than LDA and standard GGA for the calculation of band gaps in solids (see Refs. 49–55 for extensive tests) and to reach an accuracy similar to the *GW* methods.^{50,51}

Very recently,⁵⁵ GLLB-SC and mBJ band gaps of the chalcopyrite, kesterite, and wurtzite polymorphs of II-IV-V₂ and III-III-V₂ semiconductors were compared. It was shown that in most cases the GLLB-SC and mBJ band gaps are rather similar, however, in a few cases rather large differences were obtained. The experimental values were not known for a sufficient number of systems to draw a clear conclusion about the relative accuracy of the GLLB-SC and mBJ methods. To our knowledge, this is the only work which reports a direct comparison between the GLLB-SC method and other semilocal potentials that were also shown to be useful for band gap calculation in solids. The aim of the present work is to provide such a comparison, and for the band gap the large test set of 76 solids considered in our recent work³⁴ has been chosen. Since the band gap is obviously not the only interesting property of a solid to consider, results for ground-state quantities like electron densities, electric field gradients, and magnetic moments will also be shown and discussed.

The paper is organized as follows. In Sec. II, a description of the methods and the computational details are given. In Sec. III, the results are presented and discussed, and in Sec. IV the summary of the work is given.

II. METHODOLOGY

We begin by describing briefly the GLLB method and its slightly modified version GLLB-SC. More details can be found in the original works^{44–46} or in a recent review.⁵⁶ The xc energy E_{xc} can be expressed with the pair-correlation function and this leads naturally to the following partitioning for the functional derivative $v_{xc,\sigma} = \delta E_{xc} / \delta \rho_\sigma$:

$$v_{xc,\sigma}(\mathbf{r}) = v_{xc,\text{hole},\sigma}(\mathbf{r}) + v_{xc,\text{resp},\sigma}(\mathbf{r}), \quad (2)$$

where the first term is twice the xc energy density per particle, $v_{xc,\text{hole},\sigma} = 2\varepsilon_{xc,\sigma} = 2(\varepsilon_{x,\sigma} + \varepsilon_c)$ with $\varepsilon_{x,\sigma}$ and ε_c defined as

$$E_{xc} = \sum_{\sigma} \int \varepsilon_{x,\sigma}(\mathbf{r}) \rho_{\sigma}(\mathbf{r}) d^3r + \int \varepsilon_c(\mathbf{r}) \rho(\mathbf{r}) d^3r, \quad (3)$$

and is called the hole term since it is the Coulomb potential produced by the xc hole. $v_{xc,\text{resp},\sigma}$ is the response term which accounts for the response of the pair correlation function to a variation in the electron density. The exchange part $v_{x,\text{hole},\sigma}$ of the hole term is the Slater potential,⁵⁷ i.e., twice the Hartree-Fock (HF) exchange energy density, which reduces to $(3/2)v_{x,\sigma}^{\text{LDA}}$ for a constant electron density, where $v_{x,\sigma}^{\text{LDA}}$ is the exchange potential for constant density [$v_{x,\text{resp},\sigma}$ reduces to $-(1/2)v_{x,\sigma}^{\text{LDA}}$ such that overall Eq. (2) recovers the LDA limit for constant density].

Neglecting correlation, Gritsenko *et al.*⁴⁵ proposed two exchange potentials based on the partitioning given by Eq. (2) which differ by the hole term. Their first potential uses the exact (i.e., Slater) hole term, while the second one uses the exchange energy density of the B88 GGA functional⁵⁸ ($v_{x,\text{hole},\sigma}^{\text{B88}} = 2\varepsilon_{x,\sigma}^{\text{B88}}$). For both potentials the exchange response term is given by

$$v_{x,\text{resp},\sigma}^{\text{GLLB}}(\mathbf{r}) = K_x \sum_{i=1}^{N_{\sigma}} \sqrt{\epsilon_{\text{H}} - \epsilon_{i\sigma}} \frac{|\psi_{i\sigma}(\mathbf{r})|^2}{\rho_{\sigma}(\mathbf{r})}, \quad (4)$$

where the sum runs over the N_{σ} occupied orbitals of spin σ , ϵ_{H} is the highest (H) occupied orbital, and K_x was either chosen to be $K_x^{\text{LDA}} = 8\sqrt{2}/(3\pi^2)$ in order to satisfy the correct LDA limit for constant electron density or determined to satisfy the virial relation for exchange.⁵⁹ Eq. (4) is a simplified and computationally faster version of the KLI⁴⁷ response term.^{45,60} In a subsequent work,⁴⁶ correlation was also included in the GLLB potential. For the hole term this was done by adding $v_{c,\text{hole}}^{\text{PW91}} = 2\varepsilon_c^{\text{PW91}}$ (PW91 is the GGA from Perdew and Wang⁶¹), while for the response term K_x was replaced by K_{xc} that was determined from different schemes, e.g., satisfying the virial relation for exchange and correlation.

The GLLB-SC potential⁴⁴ uses the GGA PBEsol⁶² for the exchange hole term, but also for the total (hole plus response) correlation:

$$\begin{aligned} v_{xc,\sigma}^{\text{GLLB-SC}}(\mathbf{r}) &= 2\varepsilon_{x,\sigma}^{\text{PBEsol}}(\mathbf{r}) \\ &+ K_x^{\text{LDA}} \sum_{i=1}^{N_{\sigma}} \sqrt{\epsilon_{\text{H}} - \epsilon_{i\sigma}} \frac{|\psi_{i\sigma}(\mathbf{r})|^2}{\rho_{\sigma}(\mathbf{r})} \\ &+ v_{c,\sigma}^{\text{PBEsol}}(\mathbf{r}), \end{aligned} \quad (5)$$

where $v_{c,\sigma}^{\text{PBEsol}} = \delta E_c^{\text{PBEsol}} / \delta \rho_{\sigma}$ is the total (hole plus response) correlation potential.

The most important feature of the GLLB(-SC) potentials is to vary abruptly when the lowest (L) unoccupied orbital (ψ_{L}) starts to be occupied by an infinitesimal amount δ and leads to the replacement of ϵ_{H} by ϵ_{L}

in Eq. (4). This is the so-called step structure that is also exhibited by the exact xc potential, but not by most LDA and GGA potentials. The BJ^{25,63} and Armiento-Kümmel²⁹ potentials are examples of semilocal potentials that show such step structure. Kuisma *et al.*⁴⁴ showed that the step structure of the GLLB(-SC) potential leads to an expression for the exchange component of the derivative discontinuity that is given by (see Ref. 56 for a detailed derivation)

$$\Delta_x^{\text{GLLB(-SC)}} = \int \psi_L^*(\mathbf{r}) \left[\sum_{i=1}^{N_{\sigma_L}} K_x^{(\text{LDA})} (\sqrt{\epsilon_L - \epsilon_{i\sigma_L}} - \sqrt{\epsilon_H - \epsilon_{i\sigma_L}}) \frac{|\psi_{i\sigma_L}(\mathbf{r})|^2}{\rho_{\sigma_L}(\mathbf{r})} \right] \psi_L(\mathbf{r}) d^3r, \quad (6)$$

where σ_L is the spin of ψ_L and the integration is performed in the unit cell. It should be noted that in the case of metals, i.e., when $\epsilon_H = \epsilon_L$, Eq. (6) is zero, and therefore if Eq. (5) falsely predicts a system to be metallic (e.g., for InSb or FeO, see Sec. III), then Eq. (6) is of no use.

As underlined in Sec. I, the formally correct way to calculate the true band gap within the KS theory is to add a discontinuity to the KS band gap, and this is what is done with the GLLB(-SC) method. This is the very nice feature of GLLB(-SC), but it is also clear that this method is only half satisfying since the discontinuity is calculated only for exchange. In principle correlation effects should be much smaller than exchange, however it was shown that the xc discontinuity Δ_{xc} calculated in the random phase (RPA) OEP approximation for correlation^{15,17} is much smaller (by at least 50%) than Δ_x calculated with exact exchange (EXX) OEP. Therefore, agreement with experiment for the band gap can still not be fully justified from the formal point of view with GLLB(-SC).

For the present work, the GLLB-SC potential and its associated derivative discontinuity, Eqs. (5) and (6), have been implemented in WIEN2k,⁶⁴ which is an all-electron code based on the linearized augmented plane-wave method.^{65,66} From the technical point of view, we only mention that the sums in Eqs. (5) and (6) include both the band and core electrons. The results of calculations with the GLLB-SC potential on various properties will be compared to those obtained with other multiplicative potentials of the LDA, GGA, or meta-GGA (MGGA) type, which are the following. The LDA^{2,67} is exact for the homogenous electron gas, while Sloc (abbreviation for local Slater potential³¹) consists of an enhanced exchange LDA (compare $v_{x,\sigma}^{\text{Sloc}} = -1.67(2\rho_\sigma)^{0.3}$ to $v_{x,\sigma}^{\text{LDA}} \simeq -0.7386(2\rho_\sigma)^{1/3}$) with no correlation added. The GGAs are the xc PBE from Perdew *et al.*,¹⁸ the exchange of Engel and Vosko²³ (EV93PW91, combined with PW91 correlation⁶¹ as done previously in Ref. 26), the exchange from Armiento and Kümmel^{29,68,69} (AK13, no correlation added as done in Refs. 29 and 68), and

HLE16³² which is a modification of HCTH/407⁷⁰ (the exchange and correlation components are multiplied by 1.25 and 0.5, respectively). Note that all GGA potentials depend on ρ_σ and its first two derivatives, while the xc potential LB94 of van Leeuwen and Baerends,⁷¹ also considered in the present work, depends only on ρ_σ and its first derivative. Therefore, LB94 is neither a LDA nor a GGA, but lies in between (note that correlation in LB94 is LDA⁶⁷). The tested MGGA are the aforementioned BJ²⁵ and mBJ²⁸ potentials that are both combined with LDA for correlation⁶⁷ (BJLDA and mBJLDA). Note that the LDA and GGA potentials are obtained as functional derivative $v_{xc,\sigma} = \delta E_{xc}/\delta\rho_\sigma$ of energy functionals, while this is not the case for the GLLB-SC, LB94, and (m)BJLDA potentials.⁷²⁻⁷⁴ We also mention that among these potentials, (m)BJLDA, AK13, and LB94 were recently shown to lead to severe numerical problems in finite systems.^{75,76}

For completeness, calculations with a hybrid functional, YS-PBE0,⁷⁷ were also done. In YS-PBE0 (YS stands for Yukawa screened), the Coulomb operator in the HF exchange is exponentially screened (i.e., Yukawa potential) and it was shown⁷⁷ (see also Ref. 78) that YS-PBE0 leads to the same band gaps as the popular HSE06 from Heyd, Scuseria, and Ernzerhof^{79,80} which uses an error-function for the screening of the HF exchange. In the following, the acronym HSE06 will be used for all results that were obtained with YS-PBE0. Since hybrid functionals contain a fraction of HF exchange,⁸¹ (25% in YS-PBE0/HSE06) that is usually implemented in the gKS framework (as done in WIEN2k⁷⁷), the potential is nonmultiplicative. With nonmultiplicative potentials (a part of) the discontinuity Δ_{xc} is included in the orbital energies,^{10,82} which means that the gap CBM minus VBM should in principle be in better agreement with the experimental gap E_g . However, note that hybrid functionals are much more expensive than semilocal functionals such that they can not be applied routinely to very large systems, in particular with codes based on plane-waves basis functions.

All calculations presented in this work were done with WIEN2k and the convergence parameters of the calculations, like the size of the basis set or the number of \mathbf{k} -points for the integrations in the Brillouin zone, were chosen such that the results are well converged (e.g., within ~ 0.03 eV for the band gap). The solids of the test sets are listed in Table S1 of the Supplemental Material,⁸³ along with their space group and experimental geometry that was used for the calculations. For most calculations, the deep-lying core states (those which are below the Fermi energy by at least ~ 6 Ry) were treated fully relativistically, i.e., by including spin-orbit coupling (SOC), while the band states (semicore, valence, and unoccupied) were treated at the scalar-relativistic level. The only exceptions are the results for the effective masses of III-V semiconductors, which were obtained with SOC included also for the band electrons in a second-variational step.^{84,85}

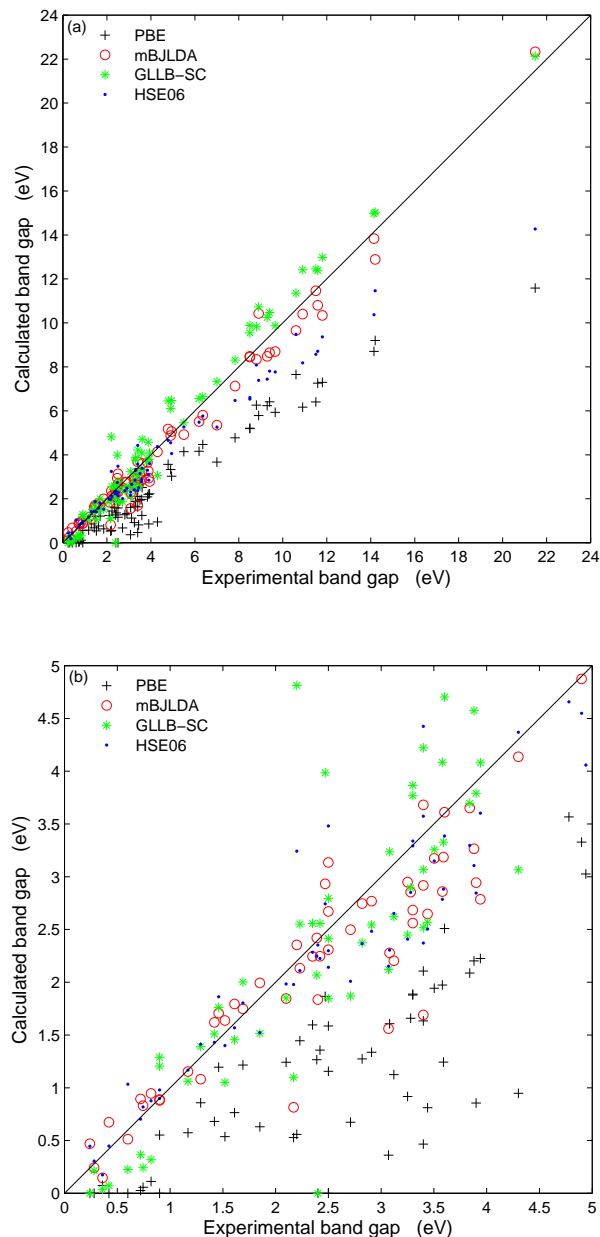


FIG. 1. Calculated versus experimental fundamental band gaps for the set of 76 solids. The values are given in Table S2 of the Supplemental Material.⁸³ The lower panel is a zoom of the upper panel focusing on band gaps smaller than 5 eV.

III. RESULTS AND DISCUSSION

A. Electronic structure

We start the discussion of the results with the fundamental band gap, whose values are shown in Table S2 of the Supplemental Material⁸³ for the 76 solids of our test set, which are of various types: *sp*-semiconductors, ionic insulators, rare gases, and strongly correlated solids. The contribution of the exchange discontinuity Δ_x to the

GLLB-SC band gap is indicated in parenthesis. The summary statistics for the error is given in Table I. Note that the results obtained with all methods except BJDLA, LB94, and GLLB-SC are from Ref. 34. The worst agreements with experiment are obtained with the standard LDA and PBE, as well as with LB94 (LB94 α ⁸⁶ leads to quite similar results on average), which strongly underestimate the band gap and lead to MAE and MARE around 2 eV and 55%, respectively, while EV93PW91 and BJDLA are slightly more accurate. Much better results are obtained with the other methods, since the MAE (MARE) of AK13, Sloc, HLE16, GLLB-SC, and the hybrid HSE06 are in the range 0.64-0.90 eV (17-30%). However, the best agreement with experiment is obtained with the mBJLDA potential, which leads to the smallest MAE (0.47 eV) and MARE (15%). As discussed in Refs. 28, 34, and 43, the very good performance of the mBJLDA potential can be attributed to its dependency on two ingredients: the kinetic-energy density $t_\sigma = (1/2) \sum_{i=1}^{N_\sigma} \nabla \psi_{i\sigma}^* \cdot \nabla \psi_{i\sigma}$, which seems particularly important for solids with strongly correlated 3d-electrons, and the average of $\nabla \rho / \rho$ in the unit cell that is able to somehow account for screening effects (see the discussion on metals in Sec. III).

The band gaps calculated with the GLLB-SC method, which consist of the sum of the KS band gap (CBM minus VBM) and the exchange discontinuity [Eq. (6)] are pretty accurate in most cases. Indeed, the MAE of 0.64 eV is smaller than the value for the hybrid functional HSE06 (and also B3PW91 which leads to 0.73 eV³⁴), and only mBJLDA has a smaller MAE. The MARE is 24%, which is a rather fair value in comparison to the other methods, since it is similar to the values for the GGAs AK13 and HLE16, but larger than what mBJLDA and HSE06 give. The ME and MRE, which are the smallest among all tested methods, indicate that GLLB-SC shows the least pronounced tendency to underestimate or overestimate the band gaps on average. However, by looking at Fig. 1, which shows graphically the band gaps for a few selected methods, we can see that there is a noticeable tendency to underestimate many of the band gaps smaller than 3 eV, while an overestimation is observed for band gaps larger than 4 eV. This is more or less the opposite of what is observed for mBJLDA, as seen in Fig. 1.

The main conclusion from the statistics in Table I for the band gap is that mBJLDA is more accurate than GLLB-SC, since the most important quantities, the MAE and MARE, are the smallest, which is also the case for the STDE and STDRE. The GLLB-SC results should also be considered as very good since the overall performance is very similar to hybrid functionals. However, note that there are some cases where GLLB-SC gives a band gap that is clearly too small, and from Fig. 1 and Table S2 we can see that this concerns mainly band gaps that are (experimentally) below 1 eV and FeO. The worst cases are InAs, InSb, SnTe, and FeO that are described as (nearly) metallic by GLLB-SC, which is in contradiction with experiment, while mBJLDA leads to reasonably

TABLE I. Summary statistics for the error in the calculated band gaps in Table S2 of the Supplemental Material⁸³ for the set of 76 solids. M(R)E, MA(R)E, and STD(R)E denote the mean (relative) error, the mean absolute (relative) error, and the standard deviation of the (relative) error, respectively. The calculations were done at the experimental geometry specified in Table S1 of the Supplemental Material.⁸³ All results except those obtained with the BJLDA, LB94, and GLLB-SC methods are taken from Ref. 34.

	LDA	PBE	EV93PW91	AK13	Sloc	HLE16	BJLDA	mBJLDA	LB94	GLLB-SC	HSE06
ME (eV)	-2.17	-1.99	-1.55	-0.28	-0.76	-0.82	-1.53	-0.30	-1.87	0.20	-0.68
MAE (eV)	2.17	1.99	1.55	0.75	0.90	0.90	1.53	0.47	1.88	0.64	0.82
STDE (eV)	1.63	1.56	1.55	0.89	0.93	1.07	1.24	0.57	1.23	0.81	1.21
MRE (%)	-58	-53	-35	-6	-21	-20	-41	-5	-54	-4	-7
MARE (%)	58	53	36	24	30	25	41	15	55	24	17
STDRE (%)	23	23	23	31	37	28	22	22	29	34	22

good results.

Concerning the strongly correlated solids, which are known to be very difficult cases for the standard functionals,⁸⁷ the GLLB-SC results seem to be particularly disparate. For Cr_2O_3 , MnO , and CoO the agreement with experiment is very good. However, as mentioned above, GLLB-SC leads to no gap in FeO (from experiment it should be around 2.4 eV) and in NiO there is an underestimation of more than 1 eV. On the other hand, the gap is 4.81 eV in Fe_2O_3 , which is too large by 2.6 eV and should be the consequence of an exchange splitting that is too large (as shown in Sec. IIIB, the magnetic moments of metals are by far overestimated). The mBJLDA potential leads to much more consistent results, since the largest discrepancy is an underestimation of about 1 eV for MnO . As mentioned in Ref. 34, all LDA and GGA methods lead to severely underestimated band gaps for the strongly correlated solids, the only exception being Sloc for MnO . LB94 is even worse since no band gap is obtained for most strongly correlated solids.

On the other hand, in Ref. 34 we underlined that mBJLDA underestimates by a rather large amount (1-1.7 eV, see Table S2) the band gap of the Cu^{1+} compounds, with CuCl being one of the worst case. For these systems, the GLLB-SC band gaps are, with respect to mBJLDA, larger by 0.3-1.3 eV such that the agreement with experiment is improved. However, with the exception of CuSCN , a sizeable underestimation is still obtained.

Discussing now the derivative discontinuity $\Delta_x^{\text{GLLB-SC}}$, Table S2 shows that its contribution to the total GLLB-SC band gap is in the range 25-35% for most solids, which is rather substantial. Without $\Delta_x^{\text{GLLB-SC}}$, the GLLB-SC band gaps would be still larger than the PBE band gaps, but clearly smaller than experiment. In Ref. 17, discontinuities were calculated in the framework of the EXX-OEP and RPA-OEP methods, and it was shown that the sum of the RPA-OEP KS band gap and $\Delta_{xc}^{\text{RPA-OEP}}$ is in relatively fair agreement with the experimental band gap for many of the solids that were considered. Thus, the order of magnitude of $\Delta_{xc}^{\text{RPA-OEP}}$ should be similar to the exact one in those cases where agreement with experiment is good. Figure 2 compares the discontinuities

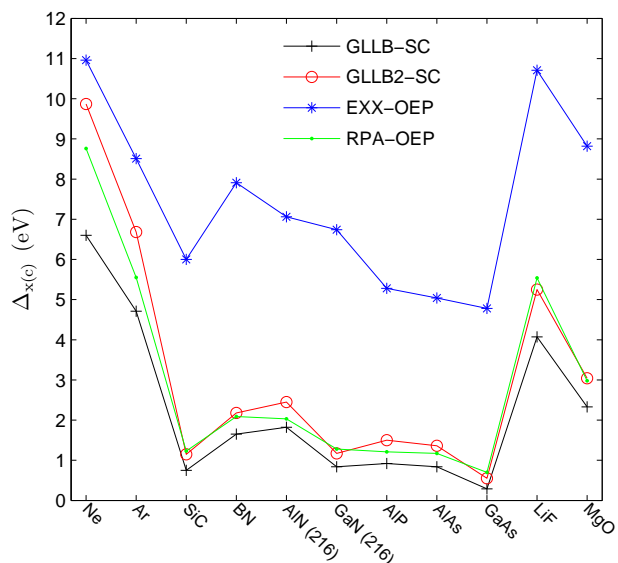


FIG. 2. GLLB-SC and GLLB2-SC derivative discontinuities compared to the values calculated in the framework of the EXX-OEP and RPA-OEP methods.¹⁷

calculated with the GLLB-SC and OEP methods, and one can clearly see that the GLLB-SC values are much closer to RPA-OEP than to EXX-OEP, despite the fact that $\Delta_x^{\text{GLLB-SC}}$ is supposed to be only for exchange. We can also see that $\Delta_x^{\text{GLLB-SC}}$ is smaller than $\Delta_{xc}^{\text{RPA-OEP}}$ by 0.2-2 eV. For the sake of consistency, it would be more preferable to have agreement with $\Delta_{xc}^{\text{RPA-OEP}}$ with a GLLB-type discontinuity which also includes correlation. As mentioned in the introduction, a (conveniently easy) way to do it was proposed in Ref. 46, and we followed a similar strategy for the construction of a potential, called GLLB2-SC, that also includes correlation in the discontinuity (see Sec. IIIE 2 for details). The values of $\Delta_{xc}^{\text{GLLB2-SC}}$, also shown in Fig. 2, show a surprisingly nice agreement with the RPA-OEP values for most solids. The largest difference between $\Delta_{xc}^{\text{GLLB2-SC}}$ and $\Delta_{xc}^{\text{RPA-OEP}}$ are found for Ne and Ar, and are about 1 eV. Nevertheless, we do not expect such a good agreement for strongly

correlated systems, since in the case of FeO, for instance, the KS band gap, and therefore the discontinuity, is still zero with GLLB2-SC. Furthermore, as discussed later in Sec. III E 2, the band gaps with GLLB2-SC are much less accurate than with the original GLLB-SC potential, such that GLLB2-SC is not really interesting for band gap calculation.

Table II shows the effective hole and electron masses of zinc-blende III-V semiconductors calculated at Γ along the ΓX [100] direction in the Brillouin zone. These semiconductors are those that we considered in Ref. 89 to compare the accuracy of various methods for effective masses. The first observation that can be made about the present results is that there is no potential which is systematically among the best ones for all systems. Nevertheless, it is still possible to make a distinction between the most and least accurate methods. By considering the number of values which show the best and worst agreement with experiment (the values in bold and underlined, respectively), as well as the cases where the effective mass can not be calculated (when the band at Γ is of nonparabolic type), the most reliable methods are EV93PW91 (11 accurate and 2 non-calculable), mBJLDA (7 accurate), HLE16 (9 accurate and 2 non-calculable), and AK13 (5 accurate and 1 inaccurate). EV93PW91 is particularly good for InP, InAs, and GaAs, HLE16 for InP, while mBJLDA and AK13 are very accurate for InSb and GaSb.

The other potentials are less accurate since as indicated in Table II, there is a (much) larger number of cases where either the value is very inaccurate or can not be calculated. For instance, in the case of the GLLB-SC potential there are 3 accurate values, 1 inaccurate, and 4 that can not be calculated. The large errors usually correspond to underestimations at the split-off-hole and light-hole VBM, while no particular trend is observed for the heavy-hole VBM and electron CBM.

To finish the discussion about the electronic structure, we show in Fig. 3 the density of states (DOS) of the ferromagnetic metal Fe. Compared to the case of $3d$ transition-metal oxides discussed above, the LDA and standard GGAs should be more reliable for itinerant transition metals where the $3d$ electrons are weakly correlated. In the case of Fe, the DOS obtained with LDA was shown to be in rather good agreement with experiment (spin-resolved X-ray photoelectron spectroscopy⁹⁰) for the valence band, and the same can be said for the PBE DOS which differs very little from the LDA DOS. However, the DOS obtained with some of the other methods differ substantially from the LDA/PBE DOS. The largest differences are obtained with GLLB-SC and HSE06, which lead to severely overestimated exchange splittings as shown in Fig. 3 and, consequently, to magnetic moments that are by far too large (see Sec. III B). The overestimation of the exchange splitting is also very large with the Sloc and HLE16 potentials. The results for Co and Ni are quite similar with an exchange splitting that is the largest with GLLB-SC and HSE06. The fail-

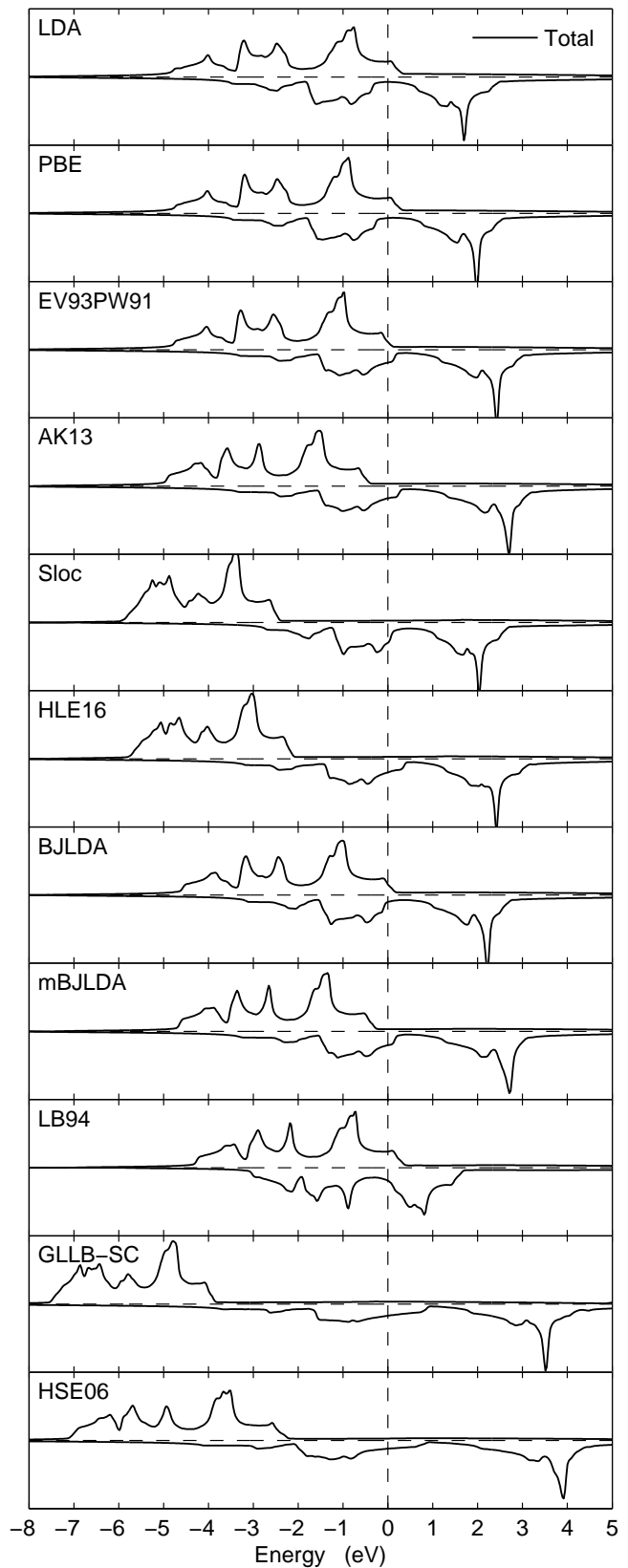


FIG. 3. Calculated spin-up (upper curve) and spin-down (lower curve) total DOS of ferromagnetic Fe. The Fermi energy is set at zero.

TABLE II. Effective hole and electron masses at the Γ point in units of the electron rest mass m_e calculated along the GX [100] direction. The calculations were done at the experimental geometry (see Table S1 of the Supplemental Material⁸³) and include SOC. The experimental values were calculated from the Luttinger parameters tabulated in Ref. 88. The values which agree the best (worst) with experiment are in bold (underlined). In some cases, because the shape of the band at Γ is of nonparabolic type, the effective mass can not be calculated.

Solid	Method	$m_{\text{split-off}}^*/m_e$	$m_{\text{light-hole}}^*/m_e$	$m_{\text{heavy-hole}}^*/m_e$	$ m_{\text{electron}}^*/m_e $
InP	LDA	<u>0.095</u>	<u>0.051</u>	<u>0.404</u>	<u>0.036</u>
	PBE	<u>0.127</u>	<u>0.073</u>	<u>0.418</u>	<u>0.052</u>
	EV93PW91	0.200	0.128	0.453	0.096
	AK13	0.250	0.170	0.489	0.138
	Sloc	<u>0.133</u>	<u>0.070</u>	0.600	<u>0.050</u>
	HLE16	0.212	0.130	0.538	0.097
	BJLDA	0.150	0.086	<u>0.427</u>	0.065
	mBJLDA	0.231	0.153	0.476	0.115
	LB94	<u>0.030</u>		<u>0.408</u>	<u>0.049</u>
	GLLB-SC	0.174	0.107	0.442	0.079
	Expt.	0.210	0.121	0.531	0.080
	InAs	LDA	<u>0.028</u>		0.317
PBE				0.324	0.036
EV93PW91		0.094	0.027	0.344	0.022
AK13		0.148	<u>0.062</u>	0.387	0.049
Sloc		<u>0.026</u>		<u>0.472</u>	<u>0.062</u>
HLE16		0.081	0.012	0.417	0.011
BJLDA		<u>0.023</u>		0.337	0.023
mBJLDA		0.132	0.053	0.368	0.041
LB94		0.104		0.338	0.200
GLLB-SC		<u>0.049</u>		0.354	
Expt.		0.140	0.027	0.333	0.026
InSb		LDA	<u>0.014</u>		<u>0.225</u>
	PBE	0.044	<u>0.111</u>	<u>0.200</u>	0.036
	EV93PW91	0.097		0.213	
	AK13	0.120	0.024	0.230	0.022
	Sloc	<u>0.030</u>		<u>0.305</u>	<u>0.094</u>
	HLE16	0.069	0.031	0.267	0.023
	BJLDA	<u>0.048</u>	<u>0.080</u>	0.211	0.034
	mBJLDA	0.114	0.020	0.229	0.018
	LB94	0.086		0.205	<u>0.213</u>
	GLLB-SC	0.060	0.033	0.210	0.023
	Expt.	0.110	0.015	0.263	0.014
	GaAs	LDA	<u>0.083</u>	<u>0.018</u>	0.331
PBE		0.111	<u>0.039</u>	0.335	<u>0.031</u>
EV93PW91		0.169	0.083	0.348	0.067
AK13		0.200	0.107	0.371	0.088
Sloc		<u>0.066</u>		<u>0.481</u>	
HLE16		0.165	0.072	0.421	0.057
BJLDA		0.135	0.056	0.351	0.044
mBJLDA		0.212	0.118	0.379	0.094
LB94		<u>0.055</u>		0.355	<u>0.107</u>
GLLB-SC		0.136	0.057	0.358	0.045
Expt.		0.172	0.090	0.350	0.067
GaSb		LDA	<u>0.057</u>	0.045	<u>0.206</u>
	PBE	0.079	0.100	<u>0.207</u>	<u>0.009</u>
	EV93PW91	0.120	0.029	0.214	0.026
	AK13	0.136	0.040	0.228	0.036
	Sloc	<u>0.011</u>	<u>0.014</u>	<u>0.313</u>	<u>0.074</u>
	HLE16	0.101		0.267	
	BJLDA	0.093		0.219	
	mBJLDA	0.148	0.051	0.235	0.045
	LB94	0.074		0.219	<u>0.188</u>
	GLLB-SC	0.089		0.213	
	Expt.	0.120	0.044	0.250	0.039

ure of hybrid functionals for Fe, Co, and Ni has already been pointed out in recent studies.^{91–94}

B. Magnetism

Turning now to the magnetic properties of systems with $3d$ electrons, Table III shows the atomic spin magnetic moment μ_S in antiferromagnetic transition-metal oxides. The comparison with experiment should be done by keeping in mind that there is a non-negligible orbital contribution μ_L for FeO, CoO, and NiO (see caption of Table III).

In addition of being particularly inaccurate to describe the electronic structure of strongly correlated solids, the LDA and commonly used GGAs like PBE also lead to magnetic moments that are too small for this class of solids.^{87,121} DFT+ U ¹²² and the hybrid functionals^{96,123–126} lead to much improved results and are therefore commonly used nowadays for such systems. However, those multiplicative potentials which are more accurate than LDA/PBE for the band gap also improve the results for the magnetic moment in most cases. From Table III we can see that in most cases, all tested potentials except LB94 increase the value of μ_S compared to LDA/PBE. EV93PW91 and BJDLD lead to moments which are only moderately larger, and AK13, Sloc, and HLE16 further improve the results, but the agreement with experiment is still not always satisfying. For instance, AK13 leads to a moment that is too small by $0.2 \mu_B$ in MnO, while too large values are obtained with Sloc and HLE16 in the case of Cr_2O_3 . GLLB-SC is pretty accurate for all monoxides, but less for Cr_2O_3 and Fe_2O_3 since the moments are overestimated by at least $0.2 \mu_B$. Overall, the most reliable multiplicative potential seems to be mBJLDA, since it is the only one which leads to an error in the magnetic moment that should be below $\sim 0.2 \mu_B$ when a quantitative comparison with experiment is possible. As already pointed out in Ref. 43, the moment of CuO obtained with mBJLDA is too large by at least $0.1 \mu_B$. Furthermore, we note that for most systems the mBJLDA results are very close to the results obtained with HSE06. The worst results are obtained with LB94 which leads to the smallest magnetic moments in all cases.

We also calculated the unit cell spin magnetic moment of the ferromagnetic metals Fe, Co, and Ni, and Table IV shows the results that are compared with experimental values that do not include the orbital component μ_L . It is well known that the simple LDA is relatively accurate for the magnetic moment of itinerant metals, while the trend of standard GGAs is to slightly overestimate the values (see Refs. 132–135 for early results on Fe, Co, and Ni).

Our results in Table IV follow the same trends observed above for the transition-metal oxides. The LDA and PBE magnetic moments are (aside from the results with LB94 and Sloc) the smallest, however, the major

difference is that for the metals, the agreement with experiment deteriorates if another potential is used, since LDA and PBE already overestimate the values (albeit slightly). For the three metals, GLLB-SC leads to magnetic moments which are by far the largest among the multiplicative potentials and too large with experiment by about 50% for Fe and Ni and 25% for Co, which is clearly worse than the overestimations obtained with the mBJLDA potential (see also Ref. 43) that are about 25% (Fe), 10% (Co), and 35% (Ni).

In Ref. 136 we showed that the screened hybrid functional YS-PBE0 (\sim HSE06) leads to a ground-state solution in fcc Rh, Pd, and Pt that is ferromagnetic instead of being nonmagnetic as determined experimentally, and the same was obtained with PBE for Pd. In general, such problems are more likely to occur with strong potentials like mBJLDA, AK13, or GLLB-SC, but probably not with LDA which is the weakest potential. For Pd for instance, the unit cell spin magnetic moment at the experimental geometry ($a = 3.887 \text{ \AA}$) is $0.25 \mu_B$ for PBE, $0.36 \mu_B$ for HLE16, $0.39\text{--}0.40 \mu_B$ for EV93PW91, AK13, and mBJLDA, and $0.44 \mu_B$ for GLLB-SC, which is similar to $0.43 \mu_B$ obtained with YS-PBE0/HSE06.¹³⁶ This ferromagnetic state is more stable than the nonmagnetic one for all these methods. No energy functional exists for mBJLDA and GLLB-SC, but independently of the one that is used to evaluate the total energy (except maybe LDA), the results show that the ferromagnetic state has a more negative total energy than the nonmagnetic one. Thus, such potentials should be used with care also in nonmagnetic metals.

In general, the use of the HF or EXX-OEP methods is not recommended for itinerant metals,^{91,92,94,136–138} since for instance, even the use of only 25% of screened HF, as in HSE06, leads to very large overestimations^{91–94} in the magnetic moment (see our HSE06 results in Table IV). Compared to GLLB-SC, the HSE06 magnetic moment is much smaller for Fe, but more similar for Co and Ni. It is only when EXX-OEP is used in combination with the RPA for correlation that reasonable values can be obtained for the magnetic moments of Fe, Co, and Ni.^{137,139} Concerning GW , a recent study reported large overestimations with self-consistent GW ,¹⁴⁰ while a good agreement with experiment was obtained with quasi-self-consistent GW .¹⁴¹

C. Electric field gradient

Now we consider the EFG, which is a measure of the accuracy of the electron density, and Table V shows the values for elemental metals and at the Cu site in CuO, Cu_2O , and Cu_2Mg . In our recent works,^{43,77,148,149} we showed that in the case of Cu_2O , the standard semilocal functionals, DFT+ U , and on-site hybrids (similar to DFT+ U) lead to magnitudes of the EFG that are by far too small compared to experiment, while the mBJLDA value is much too large. Better results could be

TABLE III. Calculated atomic spin magnetic moment μ_S (in μ_B) of antiferromagnetic 3d-transition metal oxides compared to experimental values of the total atomic magnetic moment $\mu_S + \mu_L$. The orbital moment μ_L is estimated to be in the range 0.6-1 μ_B for FeO,⁹⁵⁻⁹⁸ 1-1.6 μ_B for CoO,⁹⁵⁻¹⁰⁵ 0.3-0.45 μ_B for NiO,^{95,97,101,104,106} and much smaller in other systems. The values of μ_S are those inside the atomic sphere of radius (in bohr) 2.02 (MnO), 2.00 (FeO), 2.00 (CoO), 1.92 (NiO), 1.97 (CuO), 1.94 (Cr₂O₃), and 1.96 (Fe₂O₃) of the transition-metal atom. The calculations were done at the experimental geometry specified in Table S1 of the Supplemental Material.⁸³

Method	MnO	FeO	CoO	NiO	CuO	Cr ₂ O ₃	Fe ₂ O ₃
LDA	4.11	3.33	2.36	1.21	0.12	2.36	3.34
PBE	4.17	3.39	2.43	1.38	0.38	2.44	3.53
EV93PW91	4.24	3.44	2.49	1.47	0.46	2.53	3.71
AK13	4.39	3.51	2.59	1.57	0.54	2.68	3.93
Sloc	4.55	3.59	2.53	1.40	0.32	3.11	3.97
HLE16	4.51	3.62	2.59	1.48	0.40	2.96	4.02
BJLDA	4.19	3.40	2.48	1.48	0.50	2.43	3.59
mBJLDA	4.41	3.58	2.71	1.75	0.74	2.60	4.09
LB94	3.93	3.02	1.75	0.67	0.00	2.27	1.50
GLLB-SC	4.56	3.74	2.73	1.65	0.55	2.99	4.43
HSE06	4.36	3.55	2.65	1.68	0.67	2.61	4.08
Expt.	4.58 ^a	3.32, ^b 4.2, ^c 4.6 ^d	3.35, ^e 3.8, ^b f3.98 ^g	1.9, ^{ab} 2.2 ^{hi}	0.65 ^j	2.44, ^k 2.48, ^l 2.76 ^m	4.17, ⁿ 4.22 ^o

^a Ref. 107.

^b Ref. 108.

^c Ref. 109.

^d Ref. 110.

^e Ref. 111.

^f Ref. 112.

^g Ref. 113.

^h Ref. 106.

ⁱ Ref. 114.

^j Ref. 115.

^k Ref. 116.

^l Ref. 117.

^m Ref. 118.

ⁿ Ref. 119.

^o Ref. 120.

TABLE IV. Calculated unit cell spin magnetic moment μ_S (in μ_B /atom) of 3d-transition metals. The experimental values are also spin magnetic moments. The calculations were done at the experimental geometry specified in Table S1 of the Supplemental Material.⁸³

Method	Fe	Co	Ni
LDA	2.21	1.59	0.61
PBE	2.22	1.62	0.64
EV93PW91	2.48	1.68	0.68
AK13	2.58	1.70	0.69
Sloc	2.69	1.63	0.50
HLE16	2.72	1.72	0.63
BJLDA	2.39	1.63	0.62
mBJLDA	2.51	1.69	0.73
LB94	2.02	1.39	0.41
GLLB-SC	3.08	1.98	0.81
HSE06	2.79	1.90	0.88
Expt.	1.98, ^a 2.05, ^b 2.08 ^c	1.52, ^c 1.58, ^b d1.55-1.62 ^a	0.52, ^c 0.55 ^{be}

^a Ref. 127.

^b Ref. 128.

^c Ref. 129.

^d Ref. 130.

^e Ref. 131.

TABLE V. EFG (in 10^{21} V/m²) in elemental metals and at the Cu site in CuO, Cu₂O, and Cu₂Mg. The error bars of the experimental values are calculated from the uncertainty in the quadrupole moment and quadrupole coupling constants when available. The values which are far outside the range of experimental estimates are underlined. The calculations were done at the experimental geometry specified in Table S1 of the Supplemental Material.⁸³

Method	Ti	Zn	Zr	Tc	Ru	Cd	CuO	Cu ₂ O	Cu ₂ Mg
LDA	<u>1.80</u>	3.50	4.21	-1.65	<u>-1.56</u>	7.47	<u>-1.86</u>	<u>-5.27</u>	-5.70
PBE	1.73	3.49	4.19	-1.61	<u>-1.46</u>	7.54	<u>-2.83</u>	<u>-5.54</u>	-5.70
EV93PW91	1.61	3.43	4.13	-1.57	<u>-1.33</u>	7.63	<u>-3.17</u>	<u>-6.53</u>	-5.82
AK13	1.65	3.86	4.17	<u>-1.28</u>	-1.13	<u>8.53</u>	<u>-3.56</u>	<u>-7.92</u>	-5.44
Sloc	1.44	<u>3.93</u>	<u>2.75</u>	<u>-0.52</u>	<u>-0.35</u>	8.01	<u>-3.97</u>	-11.97	<u>-4.10</u>
HLE16	1.70	3.29	<u>3.78</u>	<u>-0.95</u>	-0.73	7.66	<u>-4.18</u>	-10.10	<u>-4.59</u>
BJLDA	<u>1.97</u>	3.51	4.25	<u>-1.27</u>	-1.16	7.61	<u>-5.42</u>	<u>-7.74</u>	-5.20
mBJLDA	<u>1.99</u>	3.35	4.33	<u>-1.20</u>	-0.90	7.56	<u>-13.93</u>	<u>-7.40</u>	<u>-4.89</u>
LB94	<u>0.94</u>	3.78	<u>1.83</u>	<u>-0.72</u>	-1.05	7.47	<u>-1.23</u>	-11.16	<u>-4.97</u>
GLLB-SC	1.62	3.72	4.42	-1.66	-1.26	8.05	<u>-4.65</u>	-9.99	-5.58
HSE06	1.5	<u>4.4</u>	4.5	-2.0	<u>-1.3</u>	<u>9.4</u>	-8.9	-8.3	<u>-6.3</u>
Expt. ^a	1.57(12)	3.40(35)	4.39(15)	1.83(9)	0.97(11)	7.60(75)	7.55(52)	10.08(69)	5.76(39)

^a Calculated using the nuclear quadrupole moments¹⁴² (in barn) of 0.302(10) (⁴⁷Ti, 5/2-), 0.220(15) (⁶³Cu, 3/2-), 0.150(15) (⁶⁷Zn, 5/2-), 0.176(3) (⁹¹Zr, 5/2+), 0.129(6) (⁹⁹Tc, 9/2+), 0.231(13) (⁹⁹Ru, 3/2+), and 0.74(7) (¹¹¹Cd, 5/2+), and the nuclear quadrupole coupling constants (in MHz) of 11.5(5) (Ti),¹⁴³ 12.34(3) (Zn),¹⁴⁴ 18.7(3) (Zr),¹⁴⁴ 5.716 (Tc),¹⁴⁴ 5.4(3) (Ru),¹⁴⁴ 136.02(41) (Cd),¹⁴⁵ 40.14 (CuO),¹⁴⁶ 53.60 (Cu₂O),¹⁴⁶ and 30.66 (Cu₂Mg).¹⁴⁷

obtained with hybrid functionals⁷⁷ or with nonstandard semilocal methods like AK13 or other variants of the BJ potential.^{148,149} In the case of CuO,⁴³ PBE and mBJLDA underestimates and overestimates significantly the EFG, respectively, while the on-site hybrid used in Ref. 150 was pretty accurate. A study by Haas and Correia¹⁵¹ on many other Cu²⁺ compounds showed that it is necessary to use DFT+*U* in order to get a reasonable agreement with experiment.

The results of the present work indicate that the GLLB-SC potential is overall the most accurate for the EFG. Indeed, it is only in the case of CuO that GLLB-SC leads to an EFG that differs noticeably from the experimental value, while all other potentials are clearly inaccurate in more than one case. Furthermore, despite that the error for CuO with GLLB-SC is rather large, it is still one of the smallest. The most inaccurate methods are LDA, Sloc, HLE16, mBJLDA, and LB94, which lead to large errors in four or five cases and are therefore not recommended for EFG calculations no matter what the system is (a semiconductor or a metal). In particular, Sloc leads to extremely large underestimation of the magnitude of the EFG in Zr, Tc, and Ru. Regarding the hybrid functional HSE06, the results for the metals seem to be reasonable for Ti, Zr, and Tc, while large errors are obtained for the others (see also Haas *et al.*¹⁵² for previous results). Thus, as mentioned above for the magnetic moment and in previous works,^{91,92,94,136} the hybrid functionals are not especially recommended for itinerant metals.

In conclusion, the GLLB-SC potential seems to be the most reliable method for the calculation of the EFG in solids. Noteworthy, in contrast to the strong overesti-

mation of the magnetic moment of Fe, Co, and Ni with GLLB-SC, the accuracy for the EFG in metals is very good and apparently superior to LDA and PBE that were supposed to lead to qualitatively correct results in metals.¹⁵³

D. Electron density of Si

The last property that we want to consider in order to judge the quality of the xc potentials is the electron density of Si, for which X-ray structure factors have been experimentally measured for the reflections from (111) to (880) and the Si form factors derived from them.^{155,156} The calculated values are given in Table S3 of the Supplemental Material⁸³ and the deviations with experiment are shown graphically in Fig. 4. As done in previous works (see, e.g., Refs. 154 and 157) the agreement with experiment is quantified in terms of *R*-factor and goodness-of-fit (GoF) (defined in the caption of Table VI). The results in Table VI show that the lowest errors, *R* = 0.10% and GoF = 5.5, are obtained with the hybrid functional HSE06. The best nonhybrid methods are PBE, EV93PW91, and BJJLDA which lead to values for *R* and GoF that are slightly larger than with HSE06. Next come LDA and mBJLDA which lead to very similar values for *R* and GoF, that are roughly two (for *R*) or three (for GoF) times larger than with PBE and EV93PW91. The most inaccurate electron densities are obtained with Sloc and HLE16, since the values for *R* and GoF are one and two orders of magnitude larger, respectively. The errors obtained with GLLB-SC are also significant since *R* = 0.75% and GoF = 240.

TABLE VI. Difference between the experimental and calculated electron densities of Si as measured by the R -factor (in %) and GoF defined as $R = 100 \sum_{i=1}^N |f_i^{\text{calc}} - f_i^{\text{exp}}| / \sum_{i=1}^N |f_i^{\text{exp}}|$ and $\text{GoF} = (1/N) \sum_{i=1}^N (f_i^{\text{calc}} - f_i^{\text{exp}})^2 / \sigma_i^2$, where the sums are over the $N = 31$ form factors f_i of Table S3 and the GoF is calculated with the average variance $\sigma = 0.0022$. The calculated form factors are multiplied by a temperature factor (see Ref. 154 for details).

Method	R	GoF
LDA	0.25	34.6
PBE	0.13	10.1
EV93PW91	0.14	12.4
AK13	0.31	67.3
Sloc	2.22	2028.9
HLE16	1.64	1087.8
BJLDA	0.16	14.1
mBJLDA	0.20	32.4
LB94	0.55	200.8
GLLB-SC	0.75	240.1
HSE06	0.10	5.5

It is also instructive to look at the form factors individually in order to have a clue about which part of the electron density (shown in Fig. 5) is described (in)accurately by a given potential. The bonding/valence region is revealed by the low-order form factors (very roughly, corresponding to $S \lesssim 0.3 \text{ \AA}^{-1}$ in Fig. 4), while the high-order ones correspond to the high density of the semicore and core electrons that are localized around the nucleus. As discussed in Ref. 154, the use of EV93 for exchange (that was combined with LDA for correlation in that work) improves the description of the core density (in particular of the $2s$ - and $2p$ -electron subshells), but deteriorates the accuracy of the bonding region compared to LDA and the GGA PW91⁶¹ (very similar to PBE). This is confirmed in Fig. 4(a), where we can see that the deviations from experiment with EV93PW91 are larger for the first five form factors, but smaller on average for the higher ones compared to LDA and PBE. An explanation for this may be that the exchange EV93 functional was fitted to the EXX-OEP in atoms, which is possibly more accurate than standard LDA/PBE for core electrons.

The mBJLDA potential [see Figs. 4(b) and 5] is quite inaccurate for the bonding region, since for the first few low-order form factors the errors are quite large, and slightly larger than with EV93PW91. However, for the (semi)core density, mBJLDA is of similar accuracy as PBE and EV93PW91, and therefore quite accurate. The GLLB-SC potential shows the opposite trend compared to mBJLDA: accurate bonding/valence electron density (small errors for the first four form factors) and very inaccurate core density (large errors for all other form factors). The HSE06 functionals leads to errors that are small for all form factors. Figure 4(c) shows that the

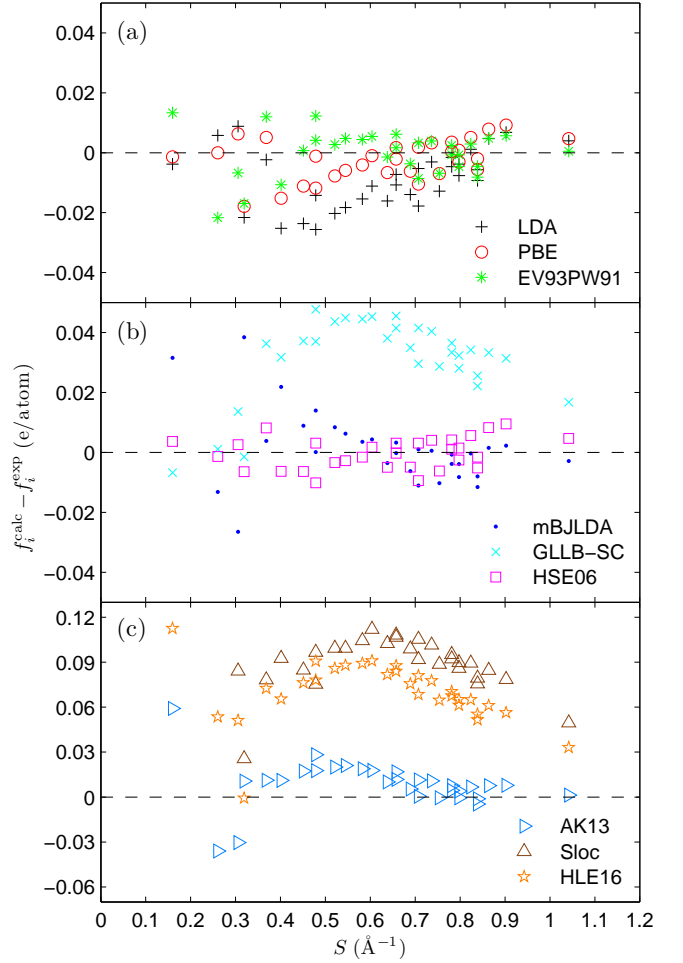


FIG. 4. Difference between the experimental and calculated form factors of Si in Table S3 plotted as a function of $S = \sin(\theta)/\lambda$. The errors with Sloc for the 1st (111) and 2nd (220) form factors are 0.22 and 0.13 e/atom, respectively, and outside the range of the y -axis range. Note that the scale of the y -axis in panel (c) is different from the one in panels (a) and (b). The results for BJD and LB94 are omitted.

Sloc and HLE16 potentials lead to extremely inaccurate electron density in general. The errors $f_i^{\text{calc}} - f_i^{\text{exp}}$ are in the range 0.05-0.12 e/atom for most form factors, while the errors with LDA, PBE, and EV93PW91 are all below 0.02 e/atom. Figure 5 shows indeed that the error in the electron density (HSE06 is chosen as the reference) with HLE16 is much larger than with PBE in the semicore and valence regions. Concerning the AK13 potential, the errors are very large for the first three form factors (i.e., the valence $3s$ and $3p$ electrons), but more or less of the same magnitude as LDA (but with opposite sign) for the others, which represent the core density.

The main conclusion of this section is that among the semilocal methods, PBE is the most accurate for the electron density of Si. The other methods are less accurate for the core and/or valence parts of the electron density.

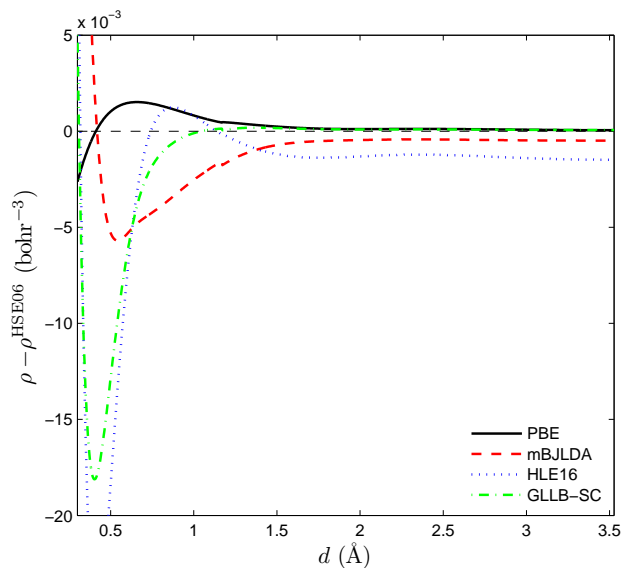


FIG. 5. Difference between the electron density ρ in Si obtained with various potentials and the one from HSE06 which is considered as the reference. The plot is along a path starting at a distance of $d = 0.3 \text{ \AA}$ from the atom at $(\frac{1}{8}, \frac{1}{8}, \frac{1}{8})$ in the direction of the center of the unit cell which is at $d = 3.527 \text{ \AA}$.

The GLLB-SC potential seems to be as accurate as PBE for the valence/bonding density, which is consistent with the observations made in Sec. III C for the EFG that is determined mainly by the valence electron density. The mBJLDA potential describes quite well the core density, but not the valence density. Overall, the best performance is obtained with the hybrid HSE06.

E. Further discussion

1. Visualization of the xc potentials

The results presented above should provide some guidance when choosing (within the KS method) an exchange-correlation potential that is adequate for the problem at hand. However, it has also been clearly shown that none of the tested potentials leads to sufficiently accurate results in all circumstances, which is hardly surprising with semilocal and hybrid methods. The search for a fast semilocal multiplicative xc potential which is more universally accurate than those presented above is certainly not an easy task. However, in this respect it may be helpful to try to understand what is going on in terms of the shape of the potentials considered in this work.

In previous works,^{26,43,148,149,158–163} trends in the results could be understood by comparing the shape of the potentials. Basically, the magnitude of the band gap and magnetic moment are directly related to the inhomogeneities in the potential, and it was observed and rationalized that more pronounced inhomogeneities fa-

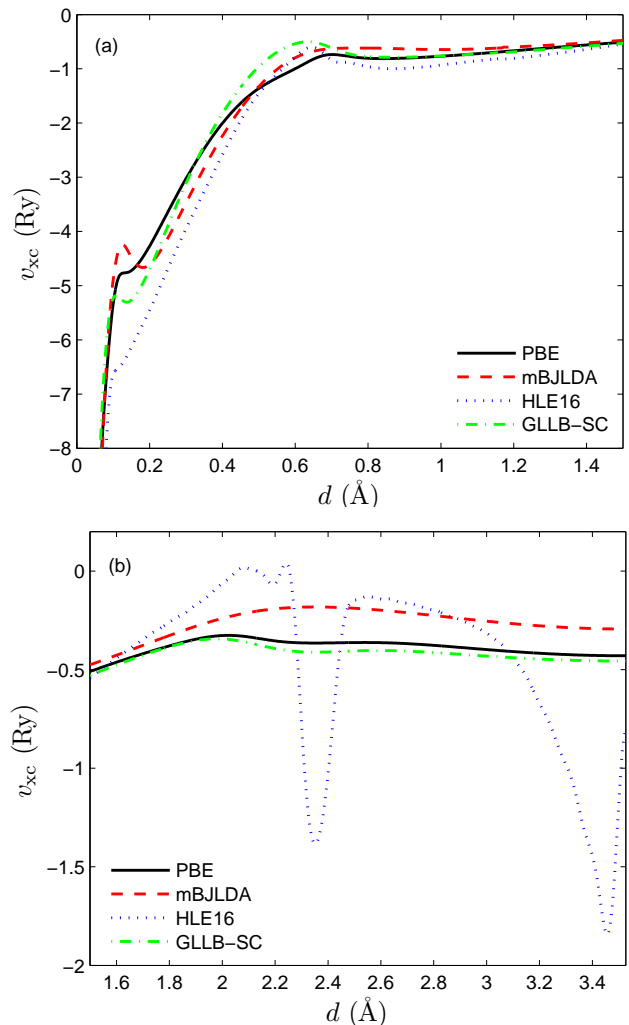


FIG. 6. Potentials v_{xc} in Si plotted from the atom at $(\frac{1}{8}, \frac{1}{8}, \frac{1}{8})$ ($d = 0$) to the center of the unit cell which is at $d = 3.527 \text{ \AA}$.

vor larger values of the band gap and magnetic moment. In order to understand some of the results discussed in the previous sections, two cases are now studied in more detail.

In Sec. III D, we showed that some of the potentials lead to very inaccurate electron density in Si. For instance, the densities obtained with Slocc, HLE16, and GLLB-SC differ quite significantly from the reference HSE06 density in the region close to the nucleus ($d \lesssim 0.7 \text{ \AA}$ in Fig. 5). Taking a look at the potentials should help us to understand the reason for this, and actually Fig. 6(a) shows that from $d = 0.1$ to 0.7 \AA the magnitudes of the HLE16 and GLLB-SC potentials (Slocc is not shown but similar) vary faster than for PBE and mBJLDA, which are much more accurate for the (semi)core density. It is this (too) fast variation in v_{xc} which leads to inaccurate density in the (semi)core region.

In our previous works,^{34,148} we showed that the nonstandard GGA potentials EV93PW91, AK13, and

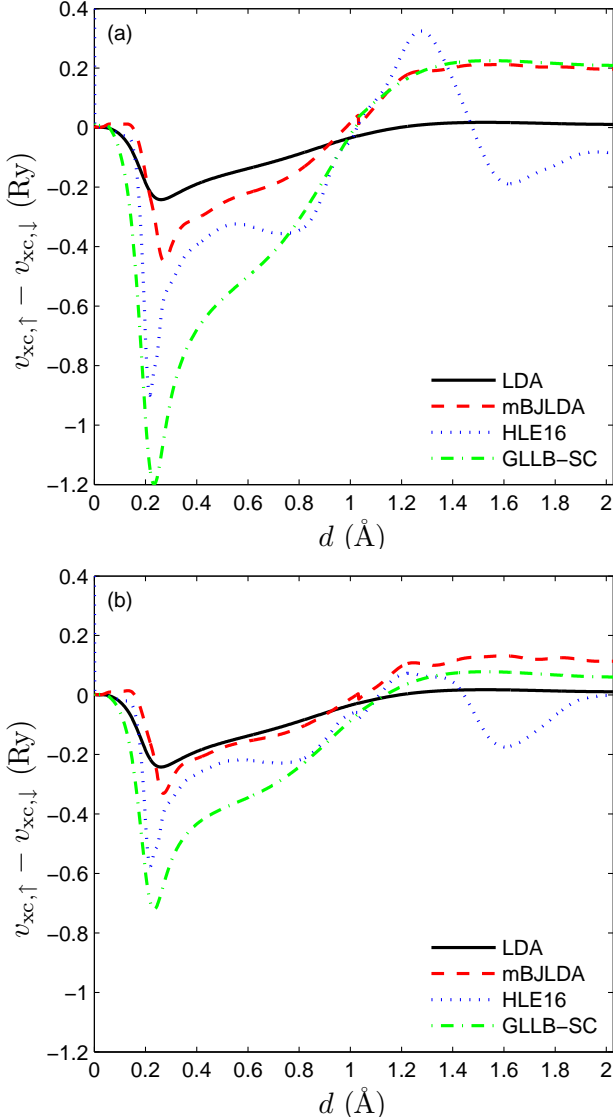


FIG. 7. $v_{xc,\uparrow} - v_{xc,\downarrow}$ in Fe plotted from the atom at $(0,0,0)$ of the body-centered cubic cell to $(\frac{1}{2}, \frac{1}{2}, 0)$ (middle of a face of the cell). (a) shows the potentials of the self-consistent calculations, while (b) shows the potentials calculated non-self-consistently using ρ_σ , t_σ , and $\psi_{i\sigma}$ from the LDA calculation.

HLE16 show large oscillations in the middle of the interstitial region [visible for d larger than 1.5 Å in Si, see Fig. 6(b)], which should mainly be a consequence of their strong dependence on the second derivative of ρ . This is not the case for the BJ-type potentials and EXX-OEP which were shown to be rather flat (as LDA and PBE) in the interstitial. The RPA-OEP also seems to be smooth according to Ref. 17. Since the GLLB-SC potential depends on the second derivative of ρ only via the correlation potential v_c^{PBEsol} , i.e. weakly, it is also smooth in the interstitial and very close to PBE (and LDA) as shown in Fig. 6(b).

One of the problems of GLLB-SC is to overestimate the exchange splitting in metals and, therefore, the mag-

netic moment in Fe, Co, and Ni. Figure 7(a) shows the difference $v_{xc,\uparrow} - v_{xc,\downarrow}$ between the self-consistent spin-up and spin-down xc potentials in Fe, where we can see that it is the largest for GLLB-SC. The large exchange splitting observed in Fig. 3 for HLE16 can also be understood from the large magnitude of $v_{xc,\uparrow} - v_{xc,\downarrow}$. Note that for $d \gtrsim 1$ Å, the mBJLDA and GLLB-SC potentials coincide very closely. Besides this, we can also see that $v_{xc,\uparrow} - v_{xc,\downarrow}$ is negative until $d \sim 1$ Å and then positive in some cases. The negative region is where the $3d$ electrons, which are the main contributors to the magnetic moment, are located, while the positive region is the interstitial where the s and p electrons, which also contribute to the magnetic moment but with opposite sign and a much smaller magnitude,^{130,131} are found. Just to give some examples, the d (d inside the atomic sphere) and sp (sp inside the atomic sphere and total from interstitial) contributions to the spin magnetic moment of Fe are 2.21 and 0.00 μ_B with LDA, 2.76 and -0.25 μ_B with mBJLDA, and 3.41 and -0.34 μ_B with GLLB-SC. Figure 7(b) also shows $v_{xc,\uparrow} - v_{xc,\downarrow}$, but this time evaluated non-self-consistently with the LDA density, orbitals, etc., where we can see that the magnitude is much smaller, indicating that the exchange splitting is strongly enhanced by the self-consistent field procedure.

2. Variants of GLLB-SC: Attempts of improvement

The results of the present and previous works^{44,49-55} have shown that the GLLB-SC potential is much more reliable for band gap calculation than all LDA and GGA methods that have been considered so far for comparison, and of quite similar accuracy as mBJLDA, the hybrids, and GW . Nevertheless, among the few problems of GLLB-SC that were pointed out, the most important are (1) a clear underestimation of most band gaps smaller than ~ 1 eV, (2) some unpredictable behavior for strongly correlated systems (for which mBJLDA is much more reliable), and (3) a very large overestimation of the magnetic moment of metals.

As said in the introduction, the idea behind the construction of the GLLB(-SC) potential is very interesting, but also very promising since it allows for a proper calculation of the band gap at a computational cost that is similar to semilocal methods. Therefore, it is certainly worth to explore further the GLLB idea, and the important question is to which extent is it possible to improve upon GLLB-SC without deteriorating the results which are already good. To try to answer this question we have considered several variants of Eq. (5), and one of the most obvious modifications consists of choosing an alternative to $2\varepsilon_{x,\sigma}^{\text{PBEsol}}$ for the exchange hole term $v_{x,\text{hole},\sigma}$, while keeping the second and third terms the same as in GLLB-SC. Among the numerous choices that we have tried for $v_{x,\text{hole},\sigma}$, three of them will be discussed, namely, $2\varepsilon_{x,\sigma}^{\text{LDA}}$, $2\varepsilon_{x,\sigma}^{\text{SCAN}}$, and $v_{x,\sigma}^{\text{BR89}}$. The latter two are MGGA since $\varepsilon_{x,\sigma}^{\text{SCAN}}$ is t_σ -dependent,¹⁶⁴ while $v_{x,\sigma}^{\text{BR89}}$ is

TABLE VII. Summary statistics for the error in the calculated band gaps in Table S4 of the Supplemental Material⁸³ for the set of 76 solids obtained with GLLB-SC and various variants which differ either in the exchange hole term, in the exchange response term, or both. The calculations were done at the experimental geometry specified in Table S1 of the Supplemental Material.⁸³

	GLLB						
	SC	LDA-x-hole	SCAN-x-hole	BR89-x-hole	PBEsol-x-resp	SCAN-x-resp	SCAN-x-hole+resp
ME (eV)	0.20	0.23	1.41	-0.24	0.55	-0.13	1.01
MAE (eV)	0.64	0.65	1.48	0.60	0.89	0.58	1.14
STDE (eV)	0.81	0.88	1.13	0.73	1.15	0.76	1.05
MRE (%)	-4	4	46	-21	6	-15	31
MARE (%)	24	22	50	28	24	26	38
STDRE (%)	34	35	56	36	33	36	47

t_σ - and $\nabla^2\rho_\sigma$ -dependent.¹⁶⁵ BR89 was constructed to be similar to the Slater potential^{163,165} and is the hole term in the BJ potential.²⁵ The results for the band gap can be found in Table S4 of the Supplemental Material⁸³ and are shown in Fig. 8, while the average errors are in Table VII. Compared to the original version of the potential, the results obtained with GLLB(LDA-x-hole) and GLLB(BR89-x-hole) are rather similar in terms of MA(R)E and STD(R)E. However, GLLB(BR89-x-hole) leads to negative M(R)E, which is due to a clear underestimation of band gaps smaller than 4 eV [see Fig. 8(b)], and actually the band gap is zero for five solids (Ge, GaSb, InAs, InSb, and VO₂), while this was the case for only two solids with GLLB-SC. The opposite trend is observed with GLLB(LDA-x-hole), which is more accurate than GLLB-SC for the band gaps smaller than ~ 1 eV, such that only one system (FeO) is described as metallic. On the other hand, the band gaps in the range 2-5 eV are more underestimated with GLLB(LDA-x-hole) than with GLLB-SC. The band gaps obtained with GLLB(SCAN-x-hole) are too large with respect to experiment and overall the results are very inaccurate since the MAE and MARE are 1.48 eV and 50%, respectively.

Thus, replacing PBEsol by something else for the exchange hole term does not really help in improving the results overall, and the same conclusion can be drawn with the other choices for $v_{x,\text{hole},\sigma}$ that we have tested (results not shown), namely, $2\varepsilon_{x,\sigma}$ of the exchange functionals EV93,²³ revTPSS,¹⁶⁶ MVS,¹⁶⁷ and TM,¹⁶⁸ with the latter three being MGGA. The general observation is that a clear improvement for a group of band gaps that are, e.g., underestimated with GLLB-SC is necessarily accompanied by a clear deterioration for another group. Also, the case of the iron oxides FeO and Fe₂O₃ is particularly problematic. While GLLB-SC leads to no band gap in FeO (experiment is 2.4 eV) and strongly overestimates the value for Fe₂O₃ (4.81 eV versus 2.2 eV for experiment), GLLB-SC(SCAN-x-hole) improves the result for FeO (0.95 eV), but overestimates even more than GLLB-SC for Fe₂O₃ (5.99 eV).

The other type of variants of Eq. (5) that we have considered consists of an exchange response term that is

multiplied by a function F_σ :

$$F_\sigma(\mathbf{r})K_x^{\text{LDA}}\sum_{i=1}^{N_\sigma}\sqrt{\epsilon_{\text{H}}-\epsilon_{i\sigma}}\frac{|\psi_{i\sigma}(\mathbf{r})|^2}{\rho_\sigma(\mathbf{r})} \quad (7)$$

and similarly in Eq. (6) for the associated derivative discontinuity. In order to be reasonable from the formal point of view, F_σ should satisfy two constraints. The first one is $F_\sigma = 1$ for a constant ρ_σ such that the potential recovers LDA as GLLB-SC does. The second constraint requires F_σ to be constructed such that the scaling property of the exchange potential¹⁶⁹ [$v_x([\rho_\lambda];\mathbf{r}) = \lambda v_x([\rho];\lambda\mathbf{r})$, where $\rho_\lambda(\mathbf{r}) = \lambda^3\rho(\lambda\mathbf{r})$] is satisfied, which is the case if F_σ depends only on the reduced density gradient $s_\sigma = |\nabla\rho_\sigma|/\left(2(6\pi^2)^{1/3}\rho_\sigma^{4/3}\right)$ for a GGA-type F_σ , and on quantities like $t_\sigma^{\text{W}}/t_\sigma$ or $t_\sigma/t_\sigma^{\text{TF}}$ for a t_σ -dependent MGGA-type F_σ [$t_\sigma^{\text{W}} = |\nabla\rho_\sigma|^2/(8\rho_\sigma)$ and $t_\sigma^{\text{TF}} = (3/10)(6\pi^2)^{2/3}\rho_\sigma^{5/3}$ are the von Weizsäcker¹⁷⁰ and Thomas-Fermi kinetic-energy density^{171,172}]. Thus, a possible choice for F_σ in Eq. (7) would be to use (blindly) any of the GGA or MGGA exchange enhancement factors $F_{x,\sigma}^{(\text{M})\text{GGA}} = \varepsilon_{x,\sigma}^{(\text{M})\text{GGA}}/\varepsilon_{x,\sigma}^{\text{LDA}}$ that are available in the literature. Such a choice could seem quite empirical and not justified, but it should just be considered as the first attempt to improve the results by making Eq. (7) $\nabla\rho_\sigma$ - or t_σ -dependent.

The results for the band gap obtained with two different exchange enhancement factors for F_σ in Eq. (7), namely $F_{x,\sigma}^{\text{PBEsol}}$ and $F_{x,\sigma}^{\text{SCAN}}$ (as in GLLB-SC, we keep PBEsol for $v_{x,\text{hole},\sigma}$ and $v_{c,\sigma}$), are shown in Fig. 9 and Tables S4 and VII. The results are rather disappointing and the trends are similar to those discussed above when different exchange hole terms were considered. Compared to GLLB-SC, GLLB(PBEsol-x-resp) and GLLB(SCAN-x-resp) lead to band gaps which are larger and smaller, respectively. Since the direction of change in the band gap is the same in basically all cases, an improvement for the underestimated band gaps (e.g., the small ones) is associated with an overestimation for most other solids, or vice versa.

Figure 9 and Tables S4 and VII also show the results

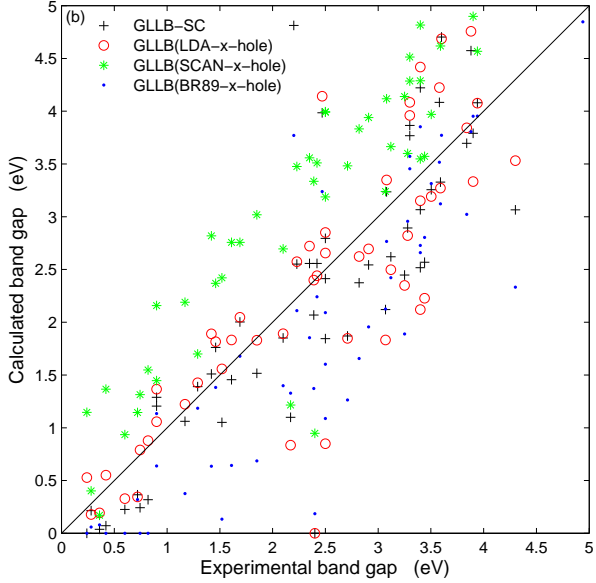
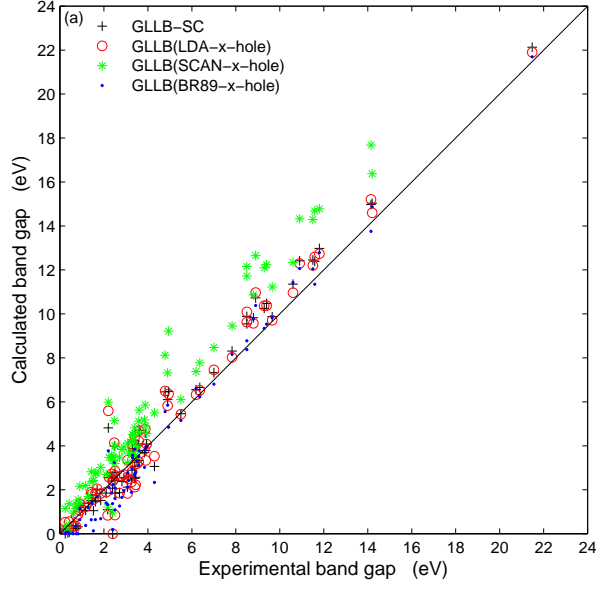


FIG. 8. Calculated versus experimental fundamental band gaps for the set of 76 solids. The calculated values were obtained with GLLB-SC and various variants which differ in the exchange hole term. The lower panel is a zoom of the upper panel focusing on band gaps smaller than 5 eV.

obtained with GLLB(SCAN-x-hole+resp) which consists of using SCAN exchange for the hole and response terms simultaneously. The accuracy of GLLB(SCAN-x-hole+resp) is in between those of GLLB(SCAN-x-hole) and GLLB(SCAN-x-resp), and overall rather low since the MAE and MARE are quite large (1.14 eV and 38%). Not shown, the results obtained with the MGGA exchange MVS¹⁶⁷ or TM¹⁶⁸ instead of SCAN for the hole and response terms indicate that TM leads to reduced errors (but still larger than GLLB-SC), while with MVS

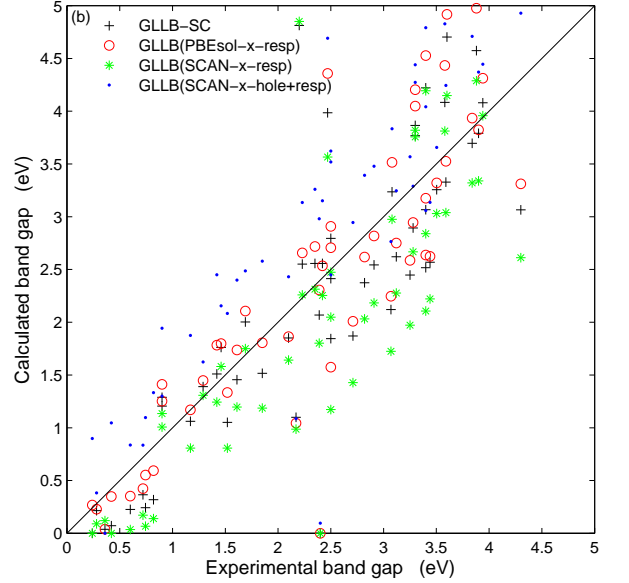
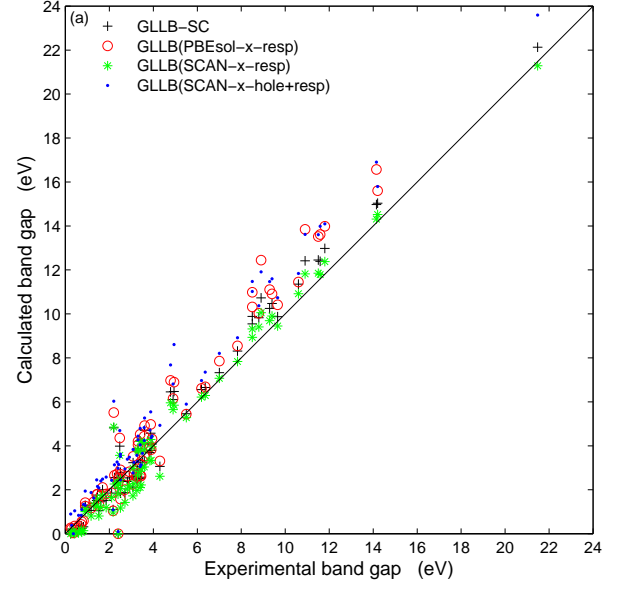


FIG. 9. Calculated versus experimental fundamental band gaps for the set of 76 solids. The calculated values were obtained with GLLB-SC and various variants which differ in the exchange response term or in both the exchange hole and response terms. The lower panel is a zoom of the upper panel focusing on band gaps smaller than 5 eV.

the errors are similar to SCAN.

The other possibilities for F_σ in Eq. (7) that we have tried are simple MGGA functions $F_\sigma = (t_\sigma/t_\sigma^{\text{TF}})^p$ or $F_\sigma = ((t_\sigma - t_\sigma^{\text{W}})/t_\sigma^{\text{TF}})^p$, which are somehow similar to the response terms $v_{x,\text{resp},\sigma}^{\text{BJ}} \propto \sqrt{t_\sigma/\rho_\sigma}$ and $v_{x,\text{resp},\sigma}^{\text{BJUC}} \propto \sqrt{(t_\sigma - t_\sigma^{\text{W}})/\rho_\sigma}$ of the BJ potential²⁵ and its gauge-invariant version (universal correction),¹⁷³ respectively. Using such functions should be promising since this is

a way to apply the GLLB idea to a potential whose response term is somehow similar to the BJ potential. However, the results that we have obtained so far with such functions F are not very encouraging and are not worth to be discussed in detail. Nevertheless, we believe that the search for such simple functions depending on the kinetic-energy density that could lead to interesting results is worth to be pursued.

The last variant of GLLB-type potential that we have considered is given by

$$v_{xc,\sigma}^{\text{GLLB2-SC}}(\mathbf{r}) = 2\varepsilon_{xc,\sigma}^{\text{PBEsol}}(\mathbf{r}) + F_{xc,\sigma}^{\text{PBEsol}}(\mathbf{r}) \times K_x^{\text{LDA}} \sum_{i=1}^{N_\sigma} \sqrt{\epsilon_{\text{H}} - \epsilon_{i\sigma}} \frac{|\psi_{i\sigma}(\mathbf{r})|^2}{\rho_\sigma(\mathbf{r})}, \quad (8)$$

where $F_{xc,\sigma}^{\text{PBEsol}} = \varepsilon_{xc,\sigma}^{\text{PBEsol}}/\varepsilon_{x,\sigma}^{\text{LDA}}$ is the total PBEsol enhancement factor.⁶² Compared to GLLB-SC [Eq. (5)], correlation is now treated the same way as exchange and, therefore, also contributes to the derivative discontinuity. Equation (8) should be considered as a simple, but still rather meaningful way to extend GLLB-SC to correlation. As discussed in Sec. III A, GLLB2-SC leads to a xc discontinuity that agrees very well with the RPA-OEP value for simple solids. However, the calculated band gaps with GLLB2-SC are quite inaccurate such that the ME and MAE are 1.35 and 1.47 eV, respectively. A large overestimation is obtained for most solids, except for those with a band gap smaller than 1 eV and a few others like FeO for which the band gap is still zero. Thus, for band gap calculation GLLB2-SC is of no interest and does not solve the problems found with GLLB-SC. Replacing PBEsol by SCAN in Eq. (8) also does not lead to any interesting improvement in the band gaps.

In this section, numerous attempts to improve upon the original GLLB-SC method have been presented. However, the results are rather disappointing since none of the variants of GLLB-SC that we have tested could really solve the problems of GLLB-SC for the band gap. We also mention that it has not been possible to really reduce the large overestimation of the magnetic moment in ferromagnetic metals compared to GLLB-SC. The fact that absolutely all variants of the GLLB-SC potential mentioned above lead to such large overestimation of μ_S strongly suggests that this problem is due to the dependency on the orbital energies ϵ_i of the second term of Eq. (5) which makes $v_{xc,\uparrow}^{\text{GLLB-SC}} - v_{xc,\downarrow}^{\text{GLLB-SC}}$ too large when $\epsilon_{i\uparrow} \neq \epsilon_{i\downarrow}$. Without entering into details, reducing the magnitude of the second term in Eq. (5) (instead of increasing it as done above) with various schemes did not lead to satisfying results. Work is under way in order to find such a scheme that reduces the exchange splitting of metals without deteriorating too much the results for other systems.

As shown above, the mBJLDA potential leads to much more balanced results for the magnetic moment (very accurate for strongly correlated solids and moderately overestimated for metals). This is mainly due to the use of the average of $\nabla\rho/\rho$ in the unit cell, which is larger in

the transition-metal oxides (1.9-1.95 bohr^{-1/2}) than in the ferromagnetic metals (1.4-1.5 bohr^{-1/2}) and therefore provides a way to make the difference between the two classes of solids (see Ref. 43 for related discussions). Thus, the use of the average of $\nabla\rho/\rho$ or another similar quantity in a GLLB-type potential should also be considered in future works.

IV. SUMMARY AND CONCLUSION

In this work, the GLLB-SC potential has been tested and compared to other methods for the description of the electronic and magnetic properties of solids, as well as properties directly related to the electron density. Concerning the band gap, GLLB-SC is, as expected, much more accurate than the LDA and GGA methods and of similar accuracy as hybrid functionals. However, GLLB-SC is on average not as accurate as mBJLDA, and the two main problems are (1) a clear underestimation of band gaps smaller than 1 eV and (2) very large variations in the error for strongly correlated solids. mBJLDA is overall less prone to large errors than GLLB-SC, in particular for the strongly correlated solids. However, mBJLDA clearly underestimates the band gap of Cu¹⁺ compounds like Cu₂O.

The magnetic moment in antiferromagnetic insulators is accurately described by GLLB-SC, mBJLDA, and the hybrid functional HSE06, while for the ferromagnetic metals GLLB-SC and HSE06 lead to very large overestimations of the magnetic moment. The mBJLDA potential also overestimates the magnetic moment in the metals, but to a much lesser extent. Concerning the EFG, it has been shown that GLLB-SC is the method leading to the best agreement with experiment, meaning that the valence electron density should be described accurately by GLLB-SC. This is, however, not the case with mBJLDA which is not recommended for EFG calculations.

Focusing on the band gap, the goal was then to improve the results with respect to GLLB-SC by modifying either the hole term or the response term (or both) in the potential. However, our numerous attempts have remained fruitless, and actually it was not possible to improve significantly the results for a group of solids (e.g., those with a small band gap) without significantly worsening the results for other compounds. This is rather disappointing, in particular since more was expected by bringing in a dependency on the kinetic-energy density into a GLLB-type potential.

Nevertheless, a multiplicative xc potential that has the same features as GLLB-SC, namely, to be computationally fast and leads to a nonzero derivative discontinuity, is ideal from the formal and practical points of view, similarly as the nonmultiplicative potentials that are functional derivatives of MGGA functionals.^{174,175} Therefore, it is certainly worth to pursue the development of such potentials, possibly by trying to incorporate more features of other successful semilocal potentials like mB-

JLDA or AK13, or by learning more from very accurate ab initio potentials.^{17,176,177} In this respect, we should remind that the mBJLDA potential uses an ingredient, the average of $\nabla\rho/\rho$ in the unit cell that has not been used in other potentials except hybrid functionals.^{11,178,179} Alternatively, the dielectric function could be used,^{179–182} however this requires the use of unoccupied orbitals. Also not yet explored, is the possibility to use the step structure of the BJ potential,⁶³ which in principle should lead to a derivative discontinuity (which is not the case with

the AK13 potential as shown in Ref. 76).

ACKNOWLEDGMENTS

This work was supported by the project F41 (SFB Vi-CoM) of the Austrian Science Fund (FWF). S.E. and P.B. acknowledge financial support from Higher Education Commission (HEC), Pakistan.

-
- ¹ P. Hohenberg and W. Kohn, Phys. Rev. **136**, B864 (1964).
² W. Kohn and L. J. Sham, Phys. Rev. **140**, A1133 (1965).
³ F. Jensen, *Introduction to Computational Chemistry, 2nd ed.* (John Wiley & Sons Ltd, Chichester, 2007).
⁴ F. Bechstedt, *Many-Body Approach to Electronic Excitations: Concepts and Applications* (Springer, Berlin Heidelberg, 2015).
⁵ M. A. L. Marques, M. J. T. Oliveira, and T. Burnus, Comput. Phys. Commun. **183**, 2272 (2012).
⁶ S. Kümmel and L. Kronik, Rev. Mod. Phys. **80**, 3 (2008).
⁷ A. J. Cohen, P. Mori-Sánchez, and W. Yang, Chem. Rev. **112**, 289 (2012).
⁸ K. Burke, J. Chem. Phys. **136**, 150901 (2012).
⁹ A. D. Becke, J. Chem. Phys. **140**, 18A301 (2014).
¹⁰ W. Yang, A. J. Cohen, and P. Mori-Sánchez, J. Chem. Phys. **136**, 204111 (2012).
¹¹ A. Seidl, A. Görling, P. Vogl, J. A. Majewski, and M. Levy, Phys. Rev. B **53**, 3764 (1996).
¹² J. P. Perdew, R. G. Parr, M. Levy, and J. L. Balduz, Jr., Phys. Rev. Lett. **49**, 1691 (1982).
¹³ L. J. Sham and M. Schlüter, Phys. Rev. Lett. **51**, 1888 (1983).
¹⁴ R. W. Godby, M. Schlüter, and L. J. Sham, Phys. Rev. Lett. **56**, 2415 (1986).
¹⁵ M. Grüning, A. Marini, and A. Rubio, J. Chem. Phys. **124**, 154108 (2006).
¹⁶ M. Grüning, A. Marini, and A. Rubio, Phys. Rev. B **74**, 161103(R) (2006).
¹⁷ J. Klimeš and G. Kresse, J. Chem. Phys. **140**, 054516 (2014).
¹⁸ J. P. Perdew, K. Burke, and M. Ernzerhof, Phys. Rev. Lett. **77**, 3865 (1996), **78**, 1396(E) (1997).
¹⁹ J. Heyd, J. E. Peralta, G. E. Scuseria, and R. L. Martin, J. Chem. Phys. **123**, 174101 (2005).
²⁰ X. Andrade and A. Aspuru-Guzik, Phys. Rev. Lett. **107**, 183002 (2011).
²¹ J.-D. Chai and P.-T. Chen, Phys. Rev. Lett. **110**, 033002 (2013).
²² E. Kraisler and L. Kronik, J. Chem. Phys. **140**, 18A540 (2014).
²³ E. Engel and S. H. Vosko, Phys. Rev. B **47**, 13164 (1993).
²⁴ G. L. Zhao, D. Bagayoko, and T. D. Williams, Phys. Rev. B **60**, 1563 (1999).
²⁵ A. D. Becke and E. R. Johnson, J. Chem. Phys. **124**, 221101 (2006).
²⁶ F. Tran, P. Blaha, and K. Schwarz, J. Phys.: Condens. Matter **19**, 196208 (2007).
²⁷ L. G. Ferreira, M. Marques, and L. K. Teles, Phys. Rev. B **78**, 125116 (2008).
²⁸ F. Tran and P. Blaha, Phys. Rev. Lett. **102**, 226401 (2009).
²⁹ R. Armiento and S. Kümmel, Phys. Rev. Lett. **111**, 036402 (2013).
³⁰ P. Singh, M. K. Harbola, M. Hemanadhan, A. Mookerjee, and D. D. Johnson, Phys. Rev. B **93**, 085204 (2016).
³¹ K. Finzel and A. I. Baranov, Int. J. Quantum Chem. **117**, 40 (2017).
³² P. Verma and D. G. Truhlar, J. Phys. Chem. Lett. **8**, 380 (2017).
³³ Á. Morales-García, R. Valero, and F. Illas, J. Phys. Chem. C **121**, 18862 (2017).
³⁴ F. Tran and P. Blaha, J. Phys. Chem. A **121**, 3318 (2017).
³⁵ D. J. Singh, Phys. Rev. B **82**, 205102 (2010).
³⁶ A. S. Botana, F. Tran, V. Pardo, D. Baldomir, and P. Blaha, Phys. Rev. B **85**, 235118 (2012).
³⁷ Z. Zhu and U. Schwingenschlögl, Phys. Rev. B **86**, 075149 (2012).
³⁸ D. Koller, F. Tran, and P. Blaha, Phys. Rev. B **85**, 155109 (2012).
³⁹ J. A. Camargo-Martínez and R. Baquero, Phys. Rev. B **86**, 195106 (2012).
⁴⁰ H. Jiang, J. Chem. Phys. **138**, 134115 (2013).
⁴¹ H. Dixit, R. Saniz, S. Cottenier, D. Lamoen, and B. Partoens, J. Phys.: Condens. Matter **24**, 205503 (2012).
⁴² D. Waroquiers, A. Lherbier, A. Miglio, M. Stankovski, S. Poncé, M. J. T. Oliveira, M. Giantomassi, G.-M. Rignanese, and X. Gonze, Phys. Rev. B **87**, 075121 (2013).
⁴³ D. Koller, F. Tran, and P. Blaha, Phys. Rev. B **83**, 195134 (2011).
⁴⁴ M. Kuisma, J. Ojanen, J. Enkovaara, and T. T. Rantala, Phys. Rev. B **82**, 115106 (2010).
⁴⁵ O. Gritsenko, R. van Leeuwen, E. van Lenthe, and E. J. Baerends, Phys. Rev. A **51**, 1944 (1995).
⁴⁶ O. V. Gritsenko, R. van Leeuwen, and E. J. Baerends, Int. J. Quantum Chem. **61**, 231 (1997).
⁴⁷ J. B. Krieger, Y. Li, and G. J. Iafrate, Phys. Rev. A **45**, 101 (1992).
⁴⁸ R. T. Sharp and G. K. Horton, Phys. Rev. **90**, 317 (1953).
⁴⁹ I. E. Castelli, T. Olsen, S. Datta, D. D. Landis, S. Dahl, K. S. Thygesen, and K. W. Jacobsen, Energy Environ. Sci. **5**, 5814 (2012).
⁵⁰ J. Yan, K. W. Jacobsen, and K. S. Thygesen, Phys. Rev. B **86**, 045208 (2012).
⁵¹ F. Hüser, T. Olsen, and K. S. Thygesen, Phys. Rev. B **87**, 235132 (2013).
⁵² P. Miró, M. Audiffred, and T. Heine, Chem. Soc. Rev. **43**, 6537 (2014).
⁵³ G. Pilania, A. Mannodi-Kanakkithodi, B. P. Uberuaga,

- R. Ramprasad, J. E. Gubernatis, and T. Lookman, *Sci. Rep.* **6**, 19375 (2016).
- ⁵⁴ C. Kim, G. Pilania, and R. Ramprasad, *J. Phys. Chem. C* **120**, 14575 (2016).
- ⁵⁵ M. Pandey, K. Kuhar, and K. W. Jacobsen, *J. Phys. Chem. C* **121**, 17780 (2017).
- ⁵⁶ E. J. Baerends, *Phys. Chem. Chem. Phys.* **19**, 15639 (2017).
- ⁵⁷ J. C. Slater, *Phys. Rev.* **81**, 385 (1951).
- ⁵⁸ A. D. Becke, *Phys. Rev. A* **38**, 3098 (1988).
- ⁵⁹ M. Levy and J. P. Perdew, *Phys. Rev. A* **32**, 2010 (1985).
- ⁶⁰ S. V. Kohut, I. G. Ryabinkin, and V. N. Staroverov, *J. Chem. Phys.* **140**, 18A535 (2014).
- ⁶¹ J. P. Perdew, J. A. Chevary, S. H. Vosko, K. A. Jackson, M. R. Pederson, D. J. Singh, and C. Fiolhais, *Phys. Rev. B* **46**, 6671 (1992), **48**, 4978(E) (1993).
- ⁶² J. P. Perdew, A. Ruzsinszky, G. I. Csonka, O. A. Vydrov, G. E. Scuseria, L. A. Constantin, X. Zhou, and K. Burke, *Phys. Rev. Lett.* **100**, 136406 (2008), **102**, 039902(E) (2009); A. E. Mattsson, R. Armiento, and T. R. Mattsson, *ibid.* **101**, 239701 (2008); J. P. Perdew, A. Ruzsinszky, G. I. Csonka, O. A. Vydrov, G. E. Scuseria, L. A. Constantin, X. Zhou, and K. Burke, *ibid.* **101**, 239702 (2008).
- ⁶³ R. Armiento, S. Kümmel, and T. Körzdörfer, *Phys. Rev. B* **77**, 165106 (2008).
- ⁶⁴ P. Blaha, K. Schwarz, G. K. H. Madsen, D. Kvasnicka, and J. Luitz, *WIEN2K: An Augmented Plane Wave plus Local Orbitals Program for Calculating Crystal Properties* (Vienna University of Technology, Austria, 2001).
- ⁶⁵ O. K. Andersen, *Phys. Rev. B* **12**, 3060 (1975).
- ⁶⁶ D. J. Singh and L. Nordström, *Planewaves, Pseudopotentials, and the LAPW Method, 2nd ed.* (Springer, New York, 2006).
- ⁶⁷ J. P. Perdew and Y. Wang, *Phys. Rev. B* **45**, 13244 (1992).
- ⁶⁸ V. Vlček, G. Steinle-Neumann, L. Leppert, R. Armiento, and S. Kümmel, *Phys. Rev. B* **91**, 035107 (2015).
- ⁶⁹ A. Lindmaa and R. Armiento, *Phys. Rev. B* **94**, 155143 (2016).
- ⁷⁰ A. D. Boese and N. C. Handy, *J. Chem. Phys.* **114**, 5497 (2001).
- ⁷¹ R. van Leeuwen and E. J. Baerends, *Phys. Rev. A* **49**, 2421 (1994).
- ⁷² A. Karolewski, R. Armiento, and S. Kümmel, *J. Chem. Theory Comput.* **5**, 712 (2009).
- ⁷³ A. P. Gaiduk and V. N. Staroverov, *J. Chem. Phys.* **131**, 044107 (2009).
- ⁷⁴ A. Karolewski, R. Armiento, and S. Kümmel, *Phys. Rev. A* **88**, 052519 (2013).
- ⁷⁵ T. Aschebrock, R. Armiento, and S. Kümmel, *Phys. Rev. B* **95**, 245118 (2017).
- ⁷⁶ T. Aschebrock, R. Armiento, and S. Kümmel, *Phys. Rev. B* **96**, 075140 (2017).
- ⁷⁷ F. Tran and P. Blaha, *Phys. Rev. B* **83**, 235118 (2011).
- ⁷⁸ T. Shimazaki and Y. Asai, *Chem. Phys. Lett.* **466**, 91 (2008).
- ⁷⁹ J. Heyd, G. E. Scuseria, and M. Ernzerhof, *J. Chem. Phys.* **118**, 8207 (2003), **124**, 219906 (2006).
- ⁸⁰ A. V. Krukau, O. A. Vydrov, A. F. Izmaylov, and G. E. Scuseria, *J. Chem. Phys.* **125**, 224106 (2006).
- ⁸¹ A. D. Becke, *J. Chem. Phys.* **98**, 5648 (1993).
- ⁸² J. P. Perdew, W. Yang, K. Burke, Z. Yang, E. K. U. Gross, M. Scheffler, G. E. Scuseria, T. M. Henderson, I. Y. Zhang, A. Ruzsinszky, H. Peng, J. Sun, E. Trushin, and A. Görling, *Proc. Natl. Acad. Sci. U.S.A.* **114**, 2801 (2017).
- ⁸³ See Supplemental Material at <http://link.aps.org/supplemental/> for information about the solids in the test set and the results for the fundamental band gap and form factors of Si.
- ⁸⁴ D. D. Koelling and B. N. Harmon, *J. Phys. C: Solid State Phys.* **10**, 3107 (1977).
- ⁸⁵ A. H. MacDonald, W. E. Pickett, and D. D. Koelling, *J. Phys. C: Solid State Phys.* **13**, 2675 (1980).
- ⁸⁶ P. R. T. Schipper, O. V. Gritsenko, S. J. A. van Gisbergen, and E. J. Baerends, *J. Chem. Phys.* **112**, 1344 (2000).
- ⁸⁷ K. Terakura, T. Oguchi, A. R. Williams, and J. Kübler, *Phys. Rev. B* **30**, 4734 (1984).
- ⁸⁸ I. Vurgaftman, J. R. Meyer, and L. R. Ram-Mohan, *J. Appl. Phys.* **89**, 5815 (2001).
- ⁸⁹ Y.-S. Kim, M. Marsman, G. Kresse, F. Tran, and P. Blaha, *Phys. Rev. B* **82**, 205212 (2010).
- ⁹⁰ A. K. See and L. E. Klebanoff, *Surf. Sci.* **340**, 309 (1995).
- ⁹¹ J. Paier, M. Marsman, K. Hummer, G. Kresse, I. C. Gerber, and J. G. Ángyán, *J. Chem. Phys.* **124**, 154709 (2006), **125**, 249901 (2006).
- ⁹² Y.-R. Jang and B. D. Yu, *J. Phys. Soc. Jpn.* **81**, 114715 (2012).
- ⁹³ P. Janthon, S. Luo, S. M. Kozlov, F. Viñes, J. Limtrakul, D. G. Truhlar, and F. Illas, *J. Chem. Theory Comput.* **10**, 3832 (2014).
- ⁹⁴ W. Gao, T. A. Abtew, T. Cai, Y.-Y. Sun, S. Zhang, and P. Zhang, *Solid State Commun.* **234-235**, 10 (2016).
- ⁹⁵ A. Svane and O. Gunnarsson, *Phys. Rev. Lett.* **65**, 1148 (1990).
- ⁹⁶ F. Tran, P. Blaha, K. Schwarz, and P. Novák, *Phys. Rev. B* **74**, 155108 (2006).
- ⁹⁷ R. J. Radwanski and Z. Ropka, *Physica B* **403**, 1453 (2008).
- ⁹⁸ A. Schrön and F. Bechstedt, *J. Phys.: Condens. Matter* **25**, 486002 (2013).
- ⁹⁹ I. V. Solovyev, A. I. Liechtenstein, and K. Terakura, *Phys. Rev. Lett.* **80**, 5758 (1998).
- ¹⁰⁰ T. Shishidou and T. Jo, *J. Phys. Soc. Jpn.* **67**, 2637 (1998).
- ¹⁰¹ W. Neubeck, C. Vettier, F. de Bergevin, F. Yakhov, D. Mannix, L. Ranno, and T. Chatterji, *J. Phys. Chem. Solids* **62**, 2173 (2001).
- ¹⁰² W. Jauch and M. Reehuis, *Phys. Rev. B* **65**, 125111 (2002).
- ¹⁰³ G. Ghiringhelli, L. H. Tjeng, A. Tanaka, O. Tjernberg, T. Mizokawa, J. L. de Boer, and N. B. Brookes, *Phys. Rev. B* **66**, 075101 (2002).
- ¹⁰⁴ R. J. Radwanski and Z. Ropka, *Physica B* **345**, 107 (2004).
- ¹⁰⁵ A. Boussendel, N. Baadji, A. Haroun, H. Dreyssé, and M. Alouani, *Phys. Rev. B* **81**, 184432 (2010).
- ¹⁰⁶ V. Fernandez, C. Vettier, F. de Bergevin, C. Giles, and W. Neubeck, *Phys. Rev. B* **57**, 7870 (1998).
- ¹⁰⁷ A. K. Cheetham and D. A. O. Hope, *Phys. Rev. B* **27**, 6964 (1983).
- ¹⁰⁸ W. L. Roth, *Phys. Rev.* **110**, 1333 (1958).
- ¹⁰⁹ P. D. Battle and A. K. Cheetham, *J. Phys. C: Solid State Phys.* **12**, 337 (1979).
- ¹¹⁰ H. Fjellvåg, F. Grønvdal, S. Stølen, and B. Hauback, *J. Solid State Chem.* **124**, 52 (1996).
- ¹¹¹ D. C. Khan and R. A. Erickson, *Phys. Rev. B* **1**, 2243 (1970).

- ¹¹² D. Herrmann-Ronzaud, P. Burlet, and J. Rossat-Mignod, *J. Phys. C: Solid State Phys.* **11**, 2123 (1978).
- ¹¹³ W. Jauch, M. Reehuis, H. J. Bleif, F. Kubanek, and P. Pattison, *Phys. Rev. B* **64**, 052102 (2001).
- ¹¹⁴ W. Neubeck, C. Vettier, V. Fernandez, F. de Bergevin, and C. Giles, *J. Appl. Phys.* **85**, 4847 (1999).
- ¹¹⁵ J. B. Forsyth, P. J. Brown, and B. M. Wanklyn, *J. Phys. C: Solid State Phys.* **21**, 2917 (1988).
- ¹¹⁶ N. O. Golosova, D. P. Kozlenko, S. E. Kichanov, E. V. Lukin, H.-P. Liermann, K. V. Glazyrin, and B. N. Savenko, *J. Alloys Compd.* **722**, 593 (2017).
- ¹¹⁷ P. J. Brown, J. B. Forsyth, E. Lelièvre-Berna, and F. Tasset, *J. Phys.: Condens. Matter* **14**, 1957 (2002).
- ¹¹⁸ L. M. Corliss, J. M. Hastings, R. Nathans, and G. Shirane, *J. Appl. Phys.* **36**, 1099 (1965).
- ¹¹⁹ V. Baron, J. Gutzmer, H. Rundlöf, and R. Tellgren, *Solid State Sci.* **7**, 753 (2005).
- ¹²⁰ A. H. Hill, F. Jiao, P. G. Bruce, A. Harrison, W. Kockelmann, and C. Ritter, *Chem. Mater.* **20**, 4891 (2008).
- ¹²¹ P. Dufek, P. Blaha, V. Sliwko, and K. Schwarz, *Phys. Rev. B* **49**, 10170 (1994).
- ¹²² V. I. Anisimov, J. Zaanen, and O. K. Andersen, *Phys. Rev. B* **44**, 943 (1991).
- ¹²³ T. Bredow and A. R. Gerson, *Phys. Rev. B* **61**, 5194 (2000).
- ¹²⁴ I. de P. R. Moreira, F. Illas, and R. L. Martin, *Phys. Rev. B* **65**, 155102 (2002).
- ¹²⁵ C. Franchini, V. Bayer, R. Podloucky, J. Paier, and G. Kresse, *Phys. Rev. B* **72**, 045132 (2005).
- ¹²⁶ M. Marsman, J. Paier, A. Stroppa, and G. Kresse, *J. Phys.: Condens. Matter* **20**, 064201 (2008).
- ¹²⁷ C. T. Chen, Y. U. Idzerda, H.-J. Lin, N. V. Smith, G. Meigs, E. Chaban, G. H. Ho, E. Pellegrin, and F. Sette, *Phys. Rev. Lett.* **75**, 152 (1995).
- ¹²⁸ A. Scherz, Ph.D. thesis, Free University of Berlin (2003).
- ¹²⁹ R. A. Reck and D. L. Fry, *Phys. Rev.* **184**, 492 (1969).
- ¹³⁰ R. M. Moon, *Phys. Rev.* **136**, A195 (1964).
- ¹³¹ H. A. Mook, *J. Appl. Phys.* **37**, 1034 (1966).
- ¹³² B. Barbiellini, E. G. Moroni, and T. Jarlborg, *J. Phys.: Condens. Matter* **2**, 7597 (1990).
- ¹³³ D. J. Singh, W. E. Pickett, and H. Krakauer, *Phys. Rev. B* **43**, 11628 (1991).
- ¹³⁴ T. C. Leung, C. T. Chan, and B. N. Harmon, *Phys. Rev. B* **44**, 2923 (1991).
- ¹³⁵ C. Amador, W. R. L. Lambrecht, and B. Segall, *Phys. Rev. B* **46**, 1870 (1992).
- ¹³⁶ F. Tran, D. Koller, and P. Blaha, *Phys. Rev. B* **86**, 134406 (2012).
- ¹³⁷ T. Kotani and H. Akai, *J. Magn. Magn. Mater.* **177-181**, 569 (1998).
- ¹³⁸ I. Schnell, G. Czycholl, and R. C. Albers, *Phys. Rev. B* **68**, 245102 (2003).
- ¹³⁹ T. Fukazawa and H. Akai, *J. Phys.: Condens. Matter* **27**, 115502 (2015).
- ¹⁴⁰ A. L. Kutepov, *J. Phys.: Condens. Matter* **29**, 465503 (2017).
- ¹⁴¹ M. van Schilfgaarde, T. Kotani, and S. Faleev, *Phys. Rev. Lett.* **96**, 226402 (2006).
- ¹⁴² N. J. Stone, *At. Data Nucl. Data Tables* **111-112**, 1 (2016).
- ¹⁴³ H. Ebert, J. Abart, and J. Voithländer, *J. Phys. F: Met. Phys.* **16**, 1287 (1986).
- ¹⁴⁴ R. Vianden, *Hyperfine Interact.* **35**, 1079 (1987).
- ¹⁴⁵ J. Christiansen, P. Heubes, R. Keitel, W. Klinger, W. Loeffler, W. Sandner, and W. Witthuhn, *Z. Phys. B* **24**, 177 (1976).
- ¹⁴⁶ R. G. Graham, P. C. Riedi, and B. M. Wanklyn, *J. Phys.: Condens. Matter* **3**, 135 (1991).
- ¹⁴⁷ L. J. Azevedo, J. E. Schirber, A. C. Switendick, R. J. Baughman, and B. Morosin, *J. Phys. F: Met. Phys.* **11**, 1521 (1981).
- ¹⁴⁸ F. Tran, P. Blaha, M. Betzinger, and S. Blügel, *Phys. Rev. B* **91**, 165121 (2015).
- ¹⁴⁹ F. Tran, P. Blaha, M. Betzinger, and S. Blügel, *Phys. Rev. B* **94**, 165149 (2016).
- ¹⁵⁰ X. Rocquefelte, M.-H. Whangbo, A. Villesuzanne, S. Jobic, F. Tran, K. Schwarz, and P. Blaha, *J. Phys.: Condens. Matter* **22**, 045502 (2010).
- ¹⁵¹ H. Haas and J. G. Correia, *Hyperfine Interact.* **176**, 9 (2007).
- ¹⁵² H. Haas, M. B. Barbosa, and J. G. Correia, *Hyperfine Interact.* **237**, 115 (2016).
- ¹⁵³ P. Blaha, K. Schwarz, and P. H. Dederichs, *Phys. Rev. B* **37**, 2792 (1988).
- ¹⁵⁴ J. M. Zuo, P. Blaha, and K. Schwarz, *J. Phys.: Condens. Matter* **9**, 7541 (1997).
- ¹⁵⁵ T. Saka and N. Kato, *Acta Cryst.* **A42**, 469 (1986).
- ¹⁵⁶ S. Cumming and M. Hart, *Aust. J. Phys.* **41**, 423 (1988).
- ¹⁵⁷ Z. W. Lu, A. Zunger, and M. Deutsch, *Phys. Rev. B* **47**, 9385 (1993).
- ¹⁵⁸ M. Städele, J. A. Majewski, P. Vogl, and A. Görling, *Phys. Rev. Lett.* **79**, 2089 (1997).
- ¹⁵⁹ M. Städele, M. Moukara, J. A. Majewski, P. Vogl, and A. Görling, *Phys. Rev. B* **59**, 10031 (1999).
- ¹⁶⁰ W. G. Aulbur, M. Städele, and A. Görling, *Phys. Rev. B* **62**, 7121 (2000).
- ¹⁶¹ A. Qteish, P. Rinke, M. Scheffler, and J. Neugebauer, *Phys. Rev. B* **74**, 245208 (2006).
- ¹⁶² M. Betzinger, C. Friedrich, S. Blügel, and A. Görling, *Phys. Rev. B* **83**, 045105 (2011).
- ¹⁶³ F. Tran, P. Blaha, and K. Schwarz, *J. Chem. Theory Comput.* **11**, 4717 (2015).
- ¹⁶⁴ J. Sun, A. Ruzsinszky, and J. P. Perdew, *Phys. Rev. Lett.* **115**, 036402 (2015).
- ¹⁶⁵ A. D. Becke and M. R. Roussel, *Phys. Rev. A* **39**, 3761 (1989).
- ¹⁶⁶ J. P. Perdew, A. Ruzsinszky, G. I. Csonka, L. A. Constantin, and J. Sun, *Phys. Rev. Lett.* **103**, 026403 (2009), **106**, 179902 (2011).
- ¹⁶⁷ J. Sun, J. P. Perdew, and A. Ruzsinszky, *Proc. Natl. Acad. Sci. U.S.A.* **112**, 685 (2015).
- ¹⁶⁸ J. Tao and Y. Mo, *Phys. Rev. Lett.* **117**, 073001 (2016).
- ¹⁶⁹ H. Ou-Yang and M. Levy, *Phys. Rev. Lett.* **65**, 1036 (1990).
- ¹⁷⁰ C. F. von Weizsäcker, *Z. Phys.* **96**, 431 (1935).
- ¹⁷¹ L. H. Thomas, *Proc. Cambridge Philos. Soc.* **23**, 542 (1927).
- ¹⁷² E. Fermi, *Rend. Accad. Naz. Lincei* **6**, 602 (1927).
- ¹⁷³ E. Räsänen, S. Pittalis, and C. R. Proetto, *J. Chem. Phys.* **132**, 044112 (2010).
- ¹⁷⁴ R. Peverati and D. G. Truhlar, *J. Chem. Phys.* **136**, 134704 (2012).
- ¹⁷⁵ Z.-h. Yang, H. Peng, J. Sun, and J. P. Perdew, *Phys. Rev. B* **93**, 205205 (2016).
- ¹⁷⁶ I. Grabowski, E. Fabiano, A. M. Teale, S. Śmiga, A. Bukstzel, and F. Della Sala, *J. Chem. Phys.* **141**, 024113 (2014).

- ¹⁷⁷ E. Ospadov, I. G. Ryabinkin, and V. N. Staroverov, *J. Chem. Phys.* **146**, 084103 (2017).
- ¹⁷⁸ D. M. Bylander and L. Kleinman, *Phys. Rev. B* **41**, 7868 (1990).
- ¹⁷⁹ M. A. L. Marques, J. Vidal, M. J. T. Oliveira, L. Reining, and S. Botti, *Phys. Rev. B* **83**, 035119 (2011).
- ¹⁸⁰ D. Koller, P. Blaha, and F. Tran, *J. Phys.: Condens. Matter* **25**, 435503 (2013).
- ¹⁸¹ J. H. Skone, M. Govoni, and G. Galli, *Phys. Rev. B* **89**, 195112 (2014).
- ¹⁸² T. Shimazaki and T. Nakajima, *J. Chem. Phys.* **142**, 074109 (2015).